2nd Annual Conference

AMERICAN SOCIETY OF BIOMECHANICS

October 25-27, 1978

The University of Michigan
Ann Arbor, Michigan

THE CONCEPTION AND EVOLUTION OF A TOTAL KNEE JOINT REPLACEMENT PROSTHESIS

Larry S. Matthews, M.D., Section of Orthopaedic Surgery,
University of Michigan Medical Center, Ann Arbor, Michigan 48109

Worldwide excitement and enthusiasm attended Borje Walldius' introduction of the first intrinsically stable knee joint replacement prosthesis in the early 1950's in Sweden. The enthusiasm melted away, however, as reports of loosening and subsequent pain and disability became more widespread in the postoperative patient population. John Charnley introduced the familiar metal on plastic, cement stabilized total hip prosthesis in the early 1960's and subsequently more than fifteen years of world experience have demonstrated the values of low friction metal on plastic bearing surfaces and methylmethacrylate prosthesis stabilization. A generation of resurfacing total knee prostheses demonstrated that the same unique developmental concepts could be utilized for the knee. All of these resurfacing prostheses, however, demanded functional ligaments. The Walldius hinge remained the only available even partially satisfactory treatment for patients with severe deformity, gross instability, or failure of a previous resurfacing arthroplasty.

We had been working for months attempting to utilize already proven materials and techniques to satisfy this recognized need when David Sonstegard proposed the seminal concept of the contained ball-in-socket main bearing articulation. Immediately, a clay model demonstrated the feasibility of the idea, and rapidly the design evolved to satisfy many of our stable knee joint design criteria: intrinsic stability, triaxial motion, metal on plastic bearing surfaces, bone-cement-metal patient-prosthesis interfaces, and soft end extension deceleration. The design improved and biomechanical tests to failure documented the stability, strength, motion, and soft end of extension. Stress coat and strain gage studies dictated final design changes to assure adequate fatigue resistance. And now, five year patient follow-ups have demonstrated that the prosthesis and operation can be of long lasting benefit to patients with severe knee joint arthritis.

We would like to emphasize the values of clearly defined objectives, of direct communication between physicians and engineers, of adequate preclinical design and materials testing, and finally of conscientious long term patient evaluations and the resultant continued evolution of the design.

THE DETERMINATION OF THREE-DIMENSIONAL KNEE STIFFNESS WITH A SONIC DIGITIZER*

Richard A. Brand, M.D.
Roy D. Crowninshield, Ph.D.
John P. Albright, M.D.

Orthopaedic Biomechanics Laboratory
University of Iowa, Iowa City, Iowa

There is a great deal of controversy about the diagnosis and treatment of knee ligament injuries. Clinical methods of evaluation and diagnosis are notoriously imprecise. Accordingly, it is difficult to compare treatment modalities in any meaningful way. Perhaps the greatest problem is our inability to quantify knee stability in any meaningful way.

In an attempt to quantify ligament stability and function, we have devised a method to study the three-dimensional stiffness (load-displacement) characteristics of cadaver knees. A table was specially constructed to hold and allow load application to cadaver knees. The specimens (fresh frozen) are cut approximately 20 centimeters above the joint line and 25 centimeters below the joint line. Skin, subcutaneous tissues, and muscle are excised except where excision could damage the joint capsule (i.e. popliteus muscle). The femur and tibia are reamed and intramedullary rods are fixed with methacrylate. The tibial rod is attached to an instrumented aluminum rod. The strain gauages are wired into a four-channel amplifier unit, which in turn is connected to a PDP12 minicomputer. The specimens are sealed in high humidity bags. Triads of noncolinear spark gaps (controlled by the minicomputer) on plastic plates are rigidly attached to the tibia and femur over the plastic bags. The specimen is then placed in the specially constructed test apparatus. The latter device allows any degree of flexion up to ninety degrees and allows either the tibia or femur to be constrained or unconstrained in any manner. Three fourteen inch orthogonal linear microphones** (sonic digitizer) are then placed over the specimen so that the two triads of spark gaps are always within its field. Computer programs control the spark gap firing on a rotating basis (one full cycle every 50 m-seconds). When a spark gap fires, the computer calculates its three-dimensional coordinates by the time intervals from firing to receiving the sound by each of the three linear microphones. During a test sequence, loads are applied manually to a knee, measured by the strain gauges and recorded by the computer. Displacements are simultaneously measured by the spark gaps and sonic digitizer and recorded by the computer. The computer automatically transfers load and displacement data to cards at the end of each test for analysis on an IMB 360 computer. Computer programs and graphics then determine and plot load-displacement curves.

The method allows the collection of large amounts of data. Intact knees are studied, then comparisons to knees with serial sectioning of ligaments allows conclusions regarding knee ligament function. The advantage of this method to those previously reported to study knee stiffness characteristics is its ability to quantitate truly three-dimensional ligament function. Sample data will be presented.

*Supported in part by funds from the Veteran's Administration and the Hearst Family Foundation.
**Graf Pen, Scientific Accessories Corporation, Stanford Connecticut.

Mechanical Aspects of Preoperative and Postoperative Muscular Performance Capabilities For Patients With Total Knee Replacement

Robert H. Deusinger, Clinical Assistant Professor,
Kinesiology/Pathokinesiology Laboratory, Department of Physical Therapy
State University of New York at Buffalo, Buffalo, New York 14214

Gary L. Smidt, Ph.D., Director and Professor, Physical Therapy Education,
University of Iowa, Iowa City, Iowa 52242

John P. Albright, M.D., Children's Hospital, Department of Orthopaedics
University of Iowa, Iowa City, Iowa, 52242

The purpose of this study was to compare pre and postoperative measurements of dynamic peak torque, work, power, and local muscular endurance of rheumatoid and degenerative arthritic patients with total knee replacements. The primary indications for total knee surgery are the presence of pain, joint deformity, and limited joint motion. Because of the large incidence of knee pathologies and disabilities, extensive efforts have been directed towards solution of the problems of pain, immobility, and deformity that confront patients with rheumatoid arthritis and degenerative arthritis. Since tibio-femoral knee implants have become a viable and prevalent surgical option as a form of treatment directed towards improvement of functional abilities, there exists a concomitant need to determine the efficacy of such treatment.

Findings of several studies have shown that post operatively most patients experience: 1) significant pain relief, 2) greater stability with less joint deformity, and 3) some improvement in range of motion. However, mechanical parameters of muscle performance that are: 1) an important aspect of the total knee replacement treatment mode, 2) necessary to human movement, and 3) associated with functional abilities have not beeen fully quantified.

Dynamic peak torque, work, power, and local muscular endurance measurements were determined from ten subjects for the knee flexors and extensors. Five of the subjects had a diagnosis of rheumatoid arthritis and five had degenerative arthritis. There were six female and four male subjects. The average age for the group was 65.9 years.

A Cybex isokinetic dynamometer served as the instrument for recording dynamic torque curves for three trials of the knee flexor and extensor muscle groups. All subjects performed at constant velocity settings of less than 30°/second. Peak torque values were determined directly from the recorded torque curves for each of the three trial contractions. Using Simpson's rule of calculus for integration, work, and power were determined for each of the three trial contractions. The experimental value for torque, work, and power was the respective mean of the three trials for each parameter. A local muscular endurance parameter was determined from a series of repetitive contractions performed during a two minute exercise bout. An ANOVA served to compare the values of the four mechanical parameters obtained preoperatively to those obtained two months and six months postoperatively.

Results show knee extensor torque to be greater preoperatively and postoperatively for the degenerative arthritics. However, the rheumatoid group appears to have improved at a relatively more rapid rate. Furthermore, by the six month post-op period both groups had achieved a power output approaching the 25ft. - lb./sec. demonstrated by normals in level walking at flatfoot. Results to date indicate a consistant improvement over time.

TIBIAL COMPONENT FIXATION OF KNEE PROSTHESES

P. S. Walker, Ph.D., D. Greene, and M. Ben-Dov, M.S.;
Howmedica, Inc., Rutherford, New Jersey 07070

The most frequent mechanical problem of 'condylar replacement' knee prostheses has been tibial component loosening. Excessive local compressive stresses on the bone, or tensile stresses at the cement-bone interface, have been cited as causes. (Walker et al, 1976; Askew et al, 1978).

For our tests, 'representative' tibial components were made as follows: modular plastic two-post, modular jointed anteriorly three-post, one-piece (no cruciate preservation) two-post, one-piece central peg: all were in plastic, and plastic in a metal tray. The plastic surfaces were cylindrical. The femoral component was a metal roller with two biconvex rollers, with partial conformity in the sagittal and frontal planes.

The rig (Fig. 1) applied any combination of compressive load, varus-valgus, a-p force, or rotation, to the femoral roller. The tibia was potted, and a metal ring cemented close to the upper surface. The bone was cut for the tibial component. The trabecular spaces on the upper surface (not the holes) were filled with clay to produce a reproducible non-tensile bond. The component was then cemented. Six linear displacement transducers were spaced around the periphery to measure the relative vertical movement between the plateau and the bone (ring). A sequence of loading and torque combinations was applied to the femoral component and displacement readings taken. After testing one plateau, it was carefully removed, and another type cemented. Three or four plateaus were used for each bone.

The results are shown for the maximum compressive load (3 body weight), the maximum anterior or posterior force (100 lbf) and the maximum internal and external torque (200 in. lbf). The numbers give the compressive (+ve) or the distraction (-ve), in units of 0.001 inch. Reproducibility was usually within 0.5 units.

In the case of two-post designs, for an anterior force, the anterior compressed and the posterior distracted. The opposite occurred for a posterior force. In rotation, there was compression and distraction diagonally opposite. The distraction reached 11 units for an anterior force and 26 units for rotation. The metal tray reduced the compressions by about 50% and the maximum distractions to only about 1 unit.

The same overall behavior occurred when a central peg design was used (Fig. 2), in that the metal tray reduced compression, particularly distraction. The two-post metal design produced more distraction than the metal central peg design, but not as much as the plastic central peg design.

Conclusions

1. The test provided a sensitive and reproducible method for measuring the relative compression and distraction between a tibial component and bone around the periphery.
2. Compressions and distractions were measured for the loading conditions of a-p force and rotations, combined with compressive loading.
3. Metal enclosed components reduced the compression and greatly reduced the distractions. This is likely to result in reduced stresses and less micromovements at the cement-bone interface, which should improve fixation.

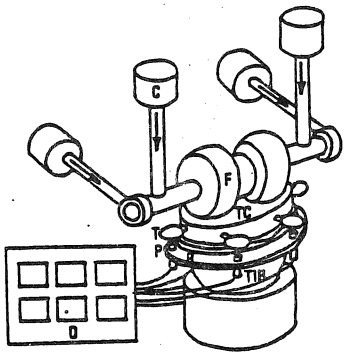

Fig. 1 The test rig. C = load cylinder; F = femoral roller: TC = tibial component: T = target, fixed to tibia: P = electronic probe, fixed to ring: R = ring: TIB = tibia: D = digital read-out.

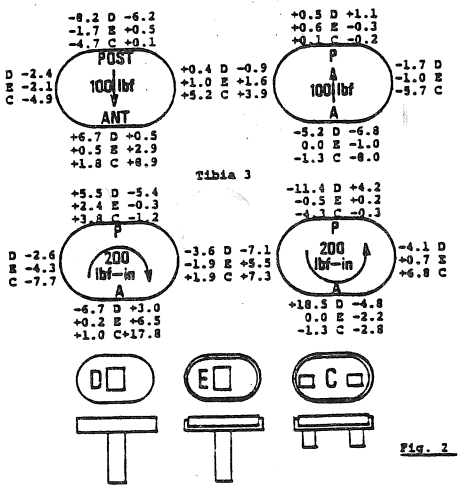

Fig. 2

References

Walker, P.S., Ranawat, C.S. and Insall, J.N.: J. Biomechanics, 9:269, 1976.

Askew, M.J., Lewis, J.L., Jaycox, D., Williams, J.L. and Hovi, R.Y.: Proc. Orthop. Research Society, Dallas, Feb. 1978.

Swimming mechanics during acceleration escape responses in crayfish Orconectes virilis.

by: Paul W. Webb
University of Michigan, School of Natural Resources, Ann Arbor, MI 48109.

High acceleration rates are characteristic of escape responses of animals including fish, cephalopods and macrurous decapod crustacea. Fish accelerate using large amplitude biphasic body and caudal fin movements. Local added mass inertial effects and a significant lift force contribute to thrust. Cephalopods accelerate using jet propulsion. Acceleration mechanics of crayfish and lobsters have not been analysed in detail.

Escape movements of crayfish were recorded on movie film at 250 frames per second, following a D.C. electric shock stimulus. Exemplary sequences of two swimming patterns were analysed; a) LG tail flips (escape responses mediated by lateral giant nerves); b) truncated tail flips used in free swimming. Velocities, angles of attack to incident flow and orientation in space were measured for propulsive segments and the center of mass.

LG tail flips were comprised of a lift-off and swimming portion, lasting 20 and 24 msec respectively. These two portions lifted the crayfish from the substrate and initiated free swimming. Truncated tail flips were analogous to the second portion of the LG tail flip and lasted 36 msec.

For both types of swimming movements, thrust generation was dominated by the telson and uropods. All propulsive segments subtended large angles of attack to the incident flow, ranging from 35 to 90°. All segments therefore generate thrust on the basis of a drag mechanism analogous to rowing.

The rate of working during the LG tail flip lift-off portion was 0.44 W for crayfish with a mean mass of 0.018 Kg. Crayfish flexor muscle was 16% of body mass, so the power output of the locomotor muscles was 147 $W.kg^{-1}$. During the LG tail flip swimming portion, energy was expended at a rate of 0.10 W, and during the truncated tail flip at 0.04 W. Since crayfish were maximally stimulated to swim and mechanical efficiency of the propulsion system must tend to unity during lift-off, the mechanical efficiency of the propulsion system must be about 0.23 and 0.10 during LG tail flip and truncated tail flip free swimming respectively.

Fish and cephalopods have about 50% locomotor muscle, half of which works at any instant for the fish. Performance of fish and cephalopods accelerating from rest is comparable to that of crayfish for similar time periods. Thus the efficiency of their propeller systems must be lower than crayfish. This is not unexpected for jet propulsion. In fish it appears that substantial energy losses are incurred through lateral recoil accelerations of the center of mass.

Low Reynolds Number Hydrodynamics and the Biology of Interstitial Animals

Donald G. Crenshaw

Department of Zoology
Duke University
Durham, North Carolina 27706

Open ocean beaches are populated by a wide variety of tiny (<1 to 5 mm long) invertebrate animals which live among the pores between sand grains. These animals are known collectively as the interstitial fauna. The action of waves and tides drives a slow oscillating flow (~0.5 mm/s) through the porous beach. The slow flow, coupled with the small size of the animals causes the animals to experience a low Reynolds number flow regime. (Reynolds number - Re = $\rho lv/\mu \approx 0.5$ where ρ is the density of water, l is the length of the animal, v is the speed of water flow, μ is the viscosity of water.) At low Reynolds number, shearing, frictional forces due to the viscosity of water and velocity gradients around the animal are relatively greater than at high Reynolds number where the pressure forces due to the density of water and rapid flow speeds predominate.

Structures and functions of animals well suited for life at low Reynolds number are quite different from the structures and functions appropriate to animals which experience high Reynolds number flow regimes.

I have studied two interstitial species which deal with water flow in contrasting ways. One species, *Tetranchyroderma bunti* is a tiny (<1 mm long) gastrotrich. It deals with flow by migrating through the beach in a manner which allows it to avoid faster flows. The other species, a turbellarian flatworm which is yet undescribed, is larger (2-3 mm long) and is found in a region of the beach where more rapid flows are common. From measurements in the laboratory of flow patterns around the animals, I estimated the force of water flow acting on the animals. *T. bunti* experiences lower forces for a given set of conditions than does the turbellarian yet adheres less strongly to the substrate. The turbellarian, though it experiences larger forces. is capable of adhering more strongly to the substrate. Further, the turbellarian is capable of altering its environment by secreting large amounts of of a highly extensible adhesive material. Under flow conditions which approximate natural conditions, this material makes the vicinity of the turbellarian a region of very slow flow. Thus the two species avoid flow caused forces by very different means.

BIOMECHANICS OF OVIDUCTAL TRANSPORT *

Anthony T. W. Cheung
Department of Biology
Loyola Marymount University
Los Angeles, California 90045

The oviduct holds a strategic position in the mammalian reproductive process; it is the only link between the ovary and the uterus and serves to provide shelter as well as transport for both the spermatozoa and ova before, during and after fertilization. The transport mechanics behind oviductal transport is extremely complicated ------ involving ciliary activity, ciliary currents, muco-ciliary interaction and muscular contractile waves (peristaltic and segmental) with varying degrees of involvement dependent on specific site locations in the oviduct.

This report deals with the overall phenomenon of ovum transport in the ampulla of mammalian oviducts from the time of ovulation to the time when the ovum reaches the ampullar-isthmic junction. For the ampullary phase of oviductal transport, the beat characteristics of oviductal cilia, the beat frequency changes with reference to the fertility and hormonal states of the mammal, the muco-ciliary interaction and the hydrodynamics of oviductal flow (and ciliary currents) are issues of fundamental importance.

Ciliary currents and muco-ciliary interaction play vital roles in the early stage of ovum transport. The freshly ovulated ovum is swept by the ciliary currents to the osteal opening of the fimbria by hormone-regulated ciliary activity. The pathways and velocities of fluid-tracers around the fimbria and in the ampullary lumen have been documented and analyzed to interpret the behavior and flow characteristics of the fluid in the ciliary flow-field. Because of the size and surface characteristics of the ovum and the morphology of the oviducts, contact between the mucoid coating of the ovum and the cilia of the oviductal epithelium is frequent throughout ampullary transport. Such contact first occurs when the ovum approaches the ostium and later occurs throughout its journey to the ampullar-isthmic junction. In-depth investigations reveal that during such contacts, the tips of the cilia actually "claw" into the mucoid coating of the ovum to render transport; to assist entrance of the ovum into the ostium in the beginning and to maintain and regulate transport at the end. This muco-ciliary interaction is quite similar to the basic mechanism found in tracheal muco-ciliary transport.

Ciliary activity is the most important single factor in initiating as well as maintaining ovum transport (in the ampullary phase of oviductal transport). The beat characteristics of oviductal cilia, the beat frequency changes with reference to the fertility and hormonal states of the mammal and the functional characteristics of the oviductal muco-ciliary interaction have been quantitatively investigated by high-speed cinemicrography under specialized optics.

A biomechanical model for oviductal transport is proposed and the overall mechanics of the ampullary phase of transport will be discussed with reference to experimentally acquired quantitative data.

* A 16mm high-speed movie will be shown with the presentation.

Energetics and mechanics of terrestrial locomotion: muscles, pendulums and springs.

C. Richard Taylor
Museum of Comparative Zoology
Harvard University
Cambridge, MA 02138

An apparent paradox has emerged from our recent studies on the energetics and mechanics of terrestrial locomotion: the metabolic energy used by animals for locomotion does not appear to be related to the mechanical work performed in the locomotion. Two examples are now well documented: 1) a 30 g mouse consumes about 20 times as much energy in moving a unit mass a unit distance as a 300 kg horse, yet the amount of mechanical work performed by the two animals is almost the same; and 2) metabolic power input for running at a constant speed increases nearly linearly with speed while mechanical power output increases curvilinearly (approximately as the square of speed). These findings are puzzling because we tend to think of muscles as biological machines which generate force, shorten, and perform mechanical work as they consume energy. We like to evaluate a muscle's performance in terms of how efficiently it converts metabolic energy into mechanical work. However, during normal locomotion, active muscles do not simply shorten. They are also active and consume significant amounts of energy while they exert force without changing length (i.e. their efficiency is zero); and while they are stretched (i.e. their efficiency is negative). These two types of muscular activity are essential for the operation of two energy conserving mechanisms involved in normal locomotion: a "pendulum-mechanism" (during a walk and a gallop); and a "spring-mechanism" (during a trot and a gallop). The limited data available on the energetics of these types of muscular activity suggests that we may be able to resolve our "paradox" by quantifying the energy involved in all these activities rather than just that used by muscles as they shorten and perform work.

QUADRUPEDAL LOCOMOTOR PATTERNS: COMPUTER-AIDED KINEMATIC ANALYSIS

J. CHARTERIS
College of Biological Science
University of Guelph
Guelph, Ontario
N1G 2W1

This paper presents a technique for analysing the angular displacements of limb segments in quadrupedal locomotion.

Recording unconstrained and hence natural gait patterns is frequently a problem for researchers of quadrupedal locomotion who use potentiometers, accelerometers, trailing wires and restrictive adhesive taping. Any method which permits freedom of movement merits sophistication and development.

The methodology here presented involves high-speed cinematography and computer-aided data reduction via a sonic digitizer. The requisite software is designed to treat the coordinates from projected frames trigonometrically, yielding the angular relationships of link segments and displaying these as Angle-vs-Angle graphs.

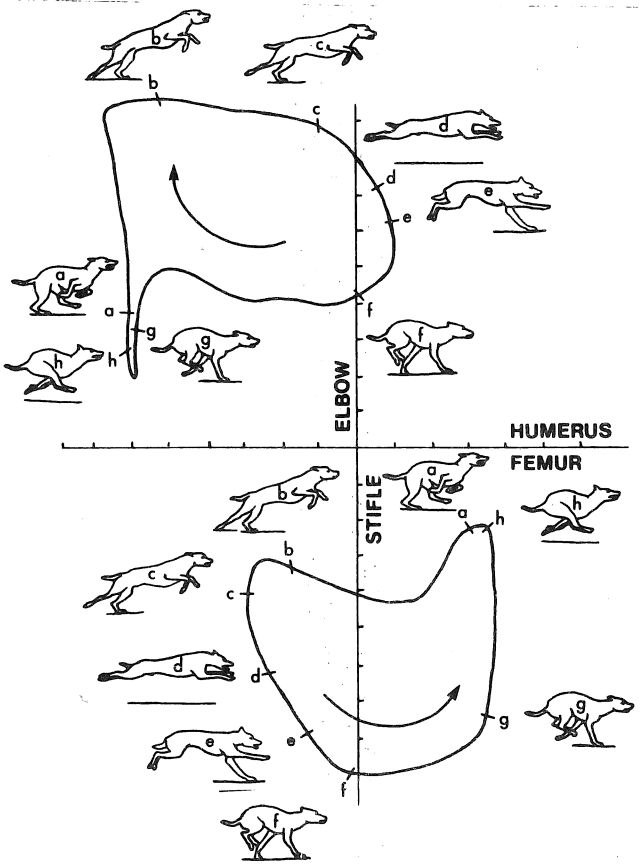

ANGLE/ANGLE DIAGRAM OF THE FORE AND HINDLIMB PATTERNS OF A GALLOPING DOG

Angle-against-time goniograms suffer the conceptual limitation of depicting a cyclic phenomenon, locomotion, in essentially linear form. Much is lost, for example, when the analysis fails to yield some understanding of the manner in which joints interact in a segmented dynamic limb to reduce the moment of inertia of the extremity during recovery. For a decade the technique of plotting the excursions of one joint against those of another, yielding cyclograms, has been known (Grieve '68), and increasingly, used in human gait analysis (Milner and Dall '73, Milner et al. '74, Sykes '75) but to date apparently no attempt has been made to apply this technique to the greater complexities of quadrupedal locomotion. The present paper shows the viability of this method of demonstrating graphically the interaction of selected key joints.

Distinctive cyclograms characterise the locomotor patterns of cursorially adapted species. Not only are inter-specific locomotor patterns dramatically differentiated, but the several locomotor styles available to a single quadrupedal species are distinguished. In the dog for example, walk, trot and gallop (and the sub-types of each of these categories) are graphically contrasted.

The clinical significance of this methodology is alluded to for those interested in the etiology and treatment of lameness in domestic species.

LOWER EXTREMITY ANGULAR DISPLACEMENT PATTERNS OF AMPUTEE RUNNERS

R.M. Enoka, D.I. Miller, E.M. Burgess, and V.H. Frankel
(University of Washington, Seattle, WA)

The running patterns of six male lower extremity amputees were analyzed. The subjects, including knee disarticulation and below-knee amputees, were chosen because of their regular participation in extra-ambulatory recreational activities. A harmonic analysis was performed on thigh and knee angular position-time data obtained from cinematographic records. The resulting functions were graphically illustrated as angle-angle diagrams.

Intact-prosthetic and amputee-normal comparisons revealed the influence of the amputation on the running gait of each individual. In general, however, within the range of running speeds recorded (2.6 to 6.8 m/s), the subjects were successful in producing periods of flight from both limbs. As running speed increased, the stride lengthened, the time devoted to support decreased, and the thigh and knee ranges of motion increased. These results were consistent with our data on skilled runners and with reports in the literature.

Although the basic shape of the angle-angle diagram was consistent for all subjects, this display proved to be sensitive to subtle alterations in the running stride (Figure 1). This analysis technique was useful in identifying the adaptations utilized by each individual in overcoming his disability. Exemplary modifications included hyperextension of the prosthetic knee during stance (to maximize stability), reduced displacement of the prosthetic heel relative to the ground prior to touchdown (to minimize the forces associated with impact), increased range of motion of the intact leg during the swing phase (to compensate for the absence of extensor musculature on the prosthetic limb), and reduced prosthetic limb extensor range of motion (in an attempt to decrease stump-socket pistoning). Despite these variations from the "normal" pattern, the present study left no doubt about the ability of lower extremity amputees to run effectively. In fact, the angle-angle diagram of one below-knee amputee running at 6.8 m/s was very similar to those derived from skilled athletes at comparable speeds.

A recent survey, in conjunction with the Prosthetics Research Study, revealed that most amputees want to participate in extra-ambulatory activities and experience a quality of life comparable to their contemporaries. Running holds the key to a physically active life for many since, as a basic locomotor skill, it is incorporated into numerous recreational pursuits.

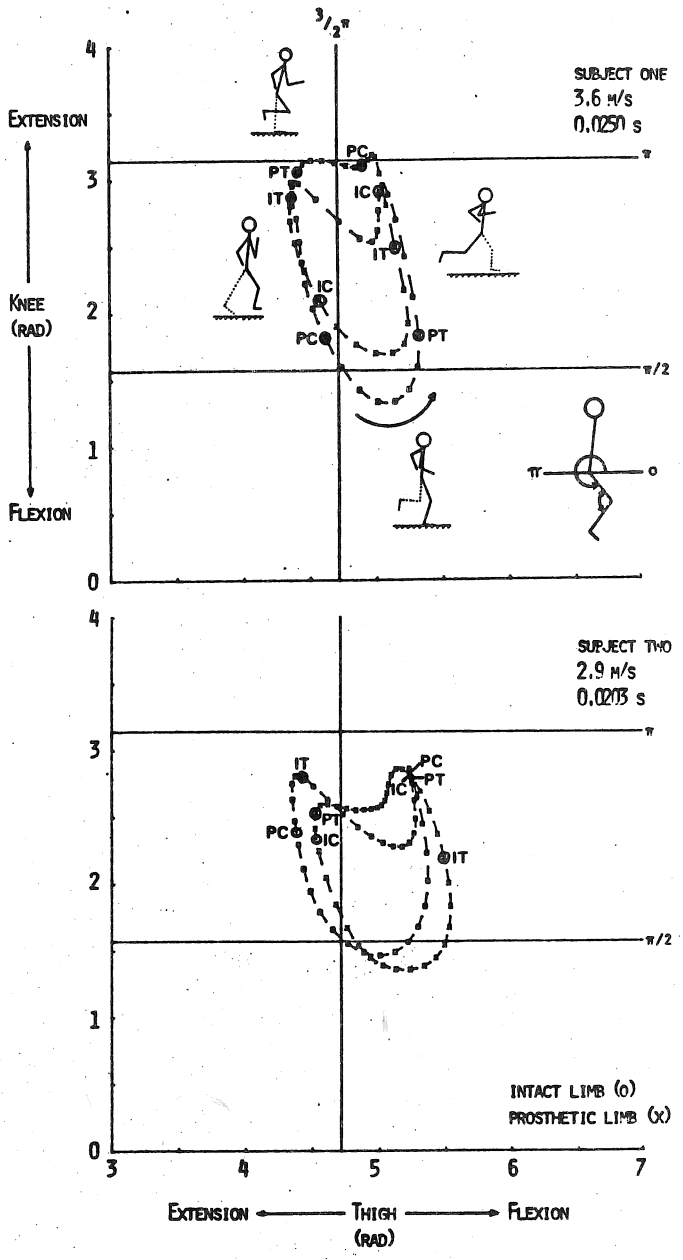

FIGURE 1. RUNNING STRIDES OF KNEE DISARTICULATION (S1) AND BELOW KNEE (S2) AMPUTEES.

Supported by VA Hospital N.Y. (Contract No. V5244P-1540) and in part by NIH Biomedical Research Support Grant RR07096.

George T. Rab, M.D.
University of California, Davis/SMC
4301 X Street
Sacramento, California 95817

FORCE AND MOTION OF THE CHILD'S HIP DURING THE GAIT CYCLE

The hip of the child is subject to an avascular necrosis, Legg-Perthes' disease, in which the proximal femoral epiphysis softens and collapses over a period of 6-18 months. Current treatment revolves around "containment" of the biologically plastic femoral head by means of a brace or surgery which keeps the head within the spherical acatebulum, ostensibly preventing deformity. This study examines the validity of the containment concept by examining the three-dimensional force and relative femoral-pelvic relationships throughout the entire gait cycle.

The three-dimensional coordinates of the acetabular rim and the perimeter of the proximal epiphysis were used to model a hemisphere rotating about three axes within a 3/4 hemisphere (the smaller acetabulum). Their relative positions during ten different phases of the gait cycle were determined, and correlated with experimental force data for each phase. The amount and location of femoral epiphysis outside the acetabulum was determined, as was the direction and magnitude of force on the remaining "contained" femoral head. The shear force on the femoral epiphyseal plate was also studied.

It was determined that x-rays of the hip in the weight-bearing position are inadequate to describe the three-dimensional kinematic behavior of the joint. The anterior and lateral femoral head, at most risk in Legg-Perthes' disease, were best "contained" at the beginning of the gait cycle (heel strike). Intra-articular force rose quickly, but reached peak at 50% of the cycle, when coverage of the anterior and lateral femoral head was the worst. Surprisingly, the joint reaction force was consistently close to the normal perpendicular to the epiphyseal line, except when that force was very small. This is interesting, since the epiphyseal cartilage is strong in compression but weak in shear.

The role of re-orientation of the acetabulum or femoral head by means of osteotomies is explored by similar analysis of the resulting relationships during the gait cycle, as is use of the abduction brace. By application of kinematic analysis, it is hoped that a more scientific approach to investigation and treatment of this complex disease can be achieved.

HEEL STRIKE
0% CYCLE

STANDARD WEIGHT-
BEARING POSITION

50% CYCLE

ONE-DIMENSIONAL MODEL OF DIASTOLIC SEMILUNAR VALVE VIBRATIONS PRODUCTIVE OF HEART SOUNDS

Edward F. Blick, Hani N. Sabbah, and Paul D. Stein

University of Oklahoma, Norman, Oklahoma and Henry Ford Hospital, Detroit, Michigan

The sound that is associated with closure of the aortic and pulmonary valves appears to result from compression and rarefaction of the blood due to vibration of the valve cusps immediately after closure. In view of the intrinsic relation of valve vibration to sound production, it is apparent that identification of the factors that affect valve vibration may clarify unexplained auscultatory observations. Therefore, this one-dimensional membrane vibration model of semilunar valve vibration was undertaken. The model assumes that the aortic valve vibrates as a circular membrane undergoing a parabolic displacement. The force that drives the membrane is assumed to be the pressure difference that acts across it. The one-degree-of-freedom equation of motion can be expressed as

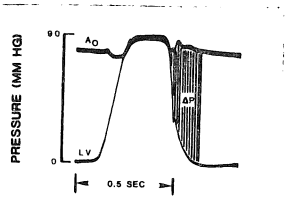

$$\ddot{m}x_o + \dot{D}x_o + Kx_o = \Delta p \pi a^2$$

where x_o is the membrane displacement at the centerline; D is the damping force coefficient; K is the stiffness factor; and Δp is the diastolic pressure gradient across the valve. To the first approximation, the pressure gradient increases linearly with time until a time, t_1, following which the pressure gradient remains essentially constant (Fig. 1). Therefore, assuming that $d\Delta p/dt$ acts as a ramp function, eq (1) can be solved by Laplace transform methods and the solution for time $t<t_1$ can be expressed as

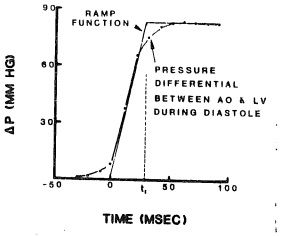

$$x_o(t) = \frac{\pi a^2}{K}\frac{d\Delta p}{dt}\left[t - \frac{2\xi}{\omega} + \frac{1}{\omega}e^{-\xi\omega_n t}\sin(\omega t-\psi)\right]$$

and the solution for $t>t_1$ is

$$x_o(t) = \frac{\pi a^2}{K}\frac{d\Delta p}{dt}\left[t_1 + \frac{1}{\omega}\left(e^{-\xi\omega_n t}\sin(\omega t-\psi) - e^{-\xi\omega_n (t-t_1)}\sin\omega\left[(t-t_1)-\psi\right]\right)\right]$$

where ω_n is the natural frequency, $\xi = D/2m\omega_n$ is the damping factor, ω is the actual frequency, and ψ the phase angle. The equation for $\dot{x}_o(t)$ can be obtained by differentiation. The theoretical curve for the one-dimensional membrane vibrational model was plotted (Fig. 2). Similarities between the calculated curves (assuming an appropriate damping force coefficient) and curves obtained from in vitro experiments are apparent. Assumptions, both of the instantaneous values of the hemodynamics that participate in valve vibration, and assumptions related to tissue characteristics of the valve were made in the solution of these equations. Therefore we view the equations as semi-quantitative. Nevertheless, the one-dimensional model of semilunar valvular vibration serves to identify physical factors that participate in valve vibration and ultimately in the production of the second heart sound. These include the valve radius, rate of change of the pressure gradient, the stiffness factor and blood viscosity (implied in the damping force coefficient).

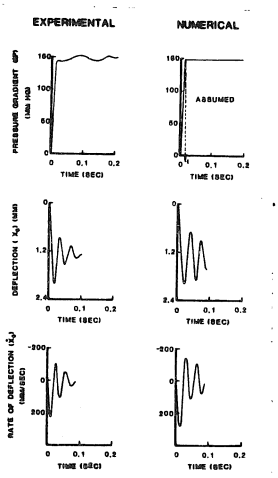

AN EXPERIMENTAL STUDY OF PULSATILE FLOW IN A CURVED TUBE

K. B. Chandran and T. L. Yearwood

Schools of Medicine and Engineering
Tulane University, New Orleans, La.

The velocity field and wall shear stress distribution due to pulsatile flow in curved tubes have been the subject of many recent investigations due to several hemodynamic theories of atherogenesis. The phenomenon of atherosclerosis is known to occur selectively at arterial curvature, bifurcation and branching sites and a better understanding of the complicated nature of blood flow at such geometries will hopefully shed more light into the origin of this disease. In this paper, the measurements of the velocity profiles due to a pulsatile flow (similar to that in the human circulatory system) of a blood-analog fluid in a curved tube is reported.

A curved tube of circular cross-section with a radius to radius of curvature ratio of 0.1 was machined out of Plexiglas® and mounted in a mock circulatory system powered by a pneumatic pump. The mock circulatory system simulates physiological pulsatile flow and the blood-analog fluid used was 50% glycerol in water which at 37° C. has a viscosity of 4 centipoise. A flow straightener was mounted in between the curved tube and the aortic valve chamber so that the fluid entering the curved tube has a flat velocity profile. Simulated blood pressure in the ventricular chamber was measured by a Statham pressure transducer and the time dependent flow rate was measured by an electromagnetic flow meter.

A flow visualization technique was used for a qualitative analysis of the flow development. In this technique, neutrally buoyant white spherical beads were suspended in the blood analog fluid and illuminated by a slit light. Flow visualization and photography were performed perpendicular to the plane of the slit light beam in the center plane of the curved tube. Both still photographic and high-speed movie recordings were made. Subsequently, holes were drilled in the center plane of the curved tube at five different stations for the insertion of the hot-film anemometry probe. The velocity profiles at these cross-sections were measured quantitatively at different times in a cycle using a Thermosystems, Inc. Constant temperature anemometer.

The results showed that during systole, the fluid in the tube accelerated downstream. In the entrance region, the maximum axial velocity was observed near the outer end of the tube. However, the maximum axial velocity shifted toward the inner end of the tube in the downstream region. During diastole, a reversed flow was observed along the inner radius of the curve with a slight forward flow along the outer radius. The velocity profiles also showed that higher magnitudes of wall shear are in general observed at the inner wall of the curve. Moreover, a large variation in the magnitude and direction of the shear stress was also observed in this region compared to the outer wall of the bend. Such variations in the distribution of wall shear stresses could be significant in the mechanism for atherogenesis.

Acknowledgement: The support of this work by a grant from the National Heart, Lung and Blood Institute (NIH), 1 R01-HL18156,is gratefully appreciated.

ASYMMETRIC FLOWS THROUGH CASCADES OF BRANCHES

B. Snyder and W. R. Debler
Dept. of Applied Mechanics, University of Michigan
Ann Arbor, Michigan 48108

Some understanding of the mechanisms through which bronchial smooth muscle regulates pulmonary air flow might be gained by observing fluid motion in simplified models. Several authors, cited in (1), have mapped point-wise flow patterns within cascades of branches, while others (2) have discovered bulk flow asymmetries arising in a two-generation planar flow section. Our intention is to observe this asymmetry effect, and the parameters which affect it, in two- and three-generation cascades, using both steady and oscillating inlet flows. We report here on our results for the case of steady flow.

Previous authors used air, which generates sizable exit losses when the flow stream encounters the atmospheric reservoir. The resulting high exit resistance would tend to damp out any asymmetry induced in the internal flow. To avoid this, we chose to use water, flowing through a planar test section composed of uniform branches, as shown in Figure 1. In the steady-state case the test section drains to atmosphere, allowing exit arm flows to be measured by timed beaker collection. This procedure is repeated with the test section rotated 180°. The results summarized in Figure 2 are derived from the average of these individual measurements.

Sizable inner-outer asymmetries have been observed at high flow rates. It is evident from Figure 2 that the (length/diameter) ratio, for which a value of 3.7 is typical of pulmonary branching, must influence the effect.

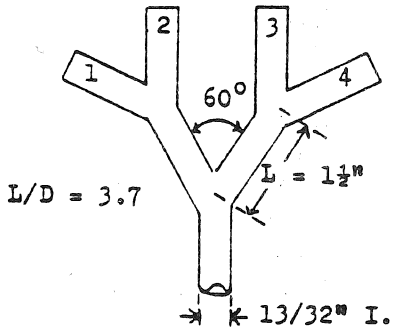

Figure 1. Two-generation flow section.

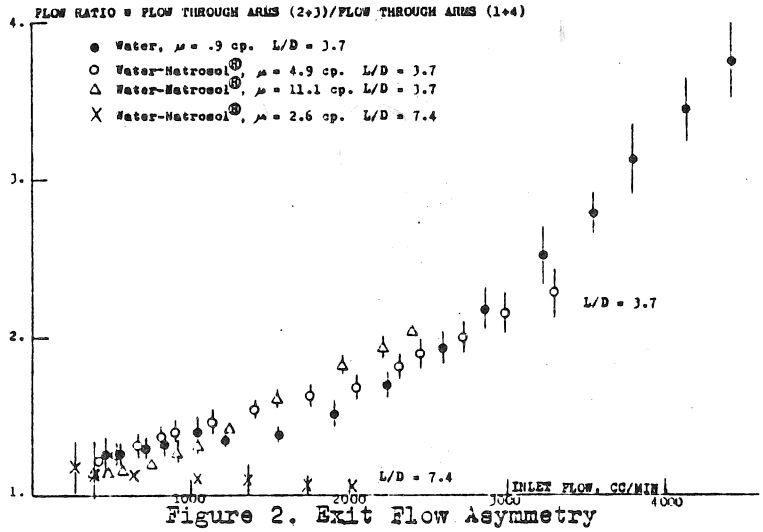

Figure 2. Exit Flow Asymmetry

1) Pedley, T.J. Pulmonary Fluid Dynamics. In: Ann. Rev. of Fluid Mech., No. 9. Annual Reviews, Inc. (Palo Alto: 1977).
2) Douglass, R.W. and Munson, B.R. J. Biomech. 7:551-7(1974).

ABSTRACT

OCCUPATIONAL BIOMECHANICS--AN EMERGING DISCIPLINE

Don B. Chaffin, Ph.D.
Professor and Chairman
Industrial and Operations Engineering
The University of Michigan

Physical trauma in the workplace is a well recognized problem in many industries. In various occupations, between 20 and 60 percent of all compensable injury and illness is classified as due to over-exertion. Slips and falls account for another 10 to 40 percent of such injury and illness. The discipline necessary to define and control the cause of such hazards is now being formulated as "Occupational Biomechanics." This paper will discuss the nature of the problem arena in industry and suggest the role that biomechanics must play to reduce such.

Four specific examples of occupational biomechanics problems are presented. These are: 1) Low-back pain resulting from strenuous exertion, 2) Carpal tunnel syndrome in repetitive hand exertions, 3) Slips when pushing and pulling objects, and 4) Falls from heights. In each case the basis for the problem is presented followed by a brief description of how biomechanics research is attempting to resolve the problem through the development of various control strategies.

USE OF OPTIMIZATION TECHNIQUES TO PREDICT MUSCLE FORCES

R. D. Crowninshield

Biomechanics Laboratory
Orthopaedic Surgery Department
University of Iowa
Iowa City, Iowa

Movement produced in the skeletal system by internally developed joint torques is the culmination of complex neurological, muscular, and skeletal function. Even the simplest of human motions is characterized by sophisticated agonistic, antagonistic, and synergistic muscle activity. The quest for basic knowledge of human physiology and efforts to treat musculoskeletal disorders have involved many attempts to mathematically describe the forces in various anatomical structures about joints. Unless gross anatomical and functional simplifications are made, the mathematical description of joint mechanics usually involve an underdetermined set of equations in which there are more unknown variables (describing muscle, ligament, and articular contact function) than there are equilibrium equations (describing intersegmental resultant force and moment). The question of ligament function is commonly dealt with by exclusion of the variables from the problem, basing ligament function on joint kinematic criteria, or by grouping individual ligament function into a single joint constraint variable. The action of antagonistic muscles is generally not considered. Having made these simplifications, the remaining problem of joint force determination is then one of redundant (synergistic) muscle activity and joint contact force.

Two basic approaches have been used to solve the indeterminate problem of predicting the force present in muscles. The first of these approaches is to reduce, by anatomic and functional simplification, the indeterminate problem to a determinate problem or to a number of determinate problems. The second commonly utilized approach to solving the indeterminate problem is that of estimating muscle forces such as to optimize (minimize or maximize) some kinetic criteria.

Presented in this paper is an adaptation of optimization methods which results in predicted muscle activity that correlates well with measured EMG activity. The adaption involves the setting of upper bound constraints on individual muscle strength that are proportional to the strenuousness of the physical activity. Determination is made of the critical muscle stress which coincides with the minimum muscle strength that permits a solution, i.e. satisfaction of the equilibrium equations. An upper bound constraint is then set at a level above this critical muscle stress.

Optimization techniques without limits on muscle strength result in the prediction of abrupt changes in muscle function as muscle moment arms change during joint rotation. The changes in muscle function can cause correspondingly abrupt changes in the magnitude and direction of the predicted joint contact force. The predicted force in a muscle may be higher than physiologically possible while the predicted joint contact force may be inappropriately low.

The technique of limiting muscle stresses to a muscle's maximum physiologically achievable stress will result in predicted synergistic activity at only higher joint moments. Discontinuities in both predicted muscle forces and joint contact force may occur.

The setting of limits on muscle stress proportional to the strenuousness of the activity encourages continuous synergistic muscle function. The synergistic activity of joint motors can be confirmed by EMG analysis. The joint contact force predicted by this method is continuous in form and of a significantly larger magnitude than that predicted by the other methods.

BIOMECHANICAL QUANTIFICATION OF PASSIVE RESISTANCE TO MOTION IN PATIENTS WITH CEREBRAL PALSY: BEFORE AND AFTER CEREBELLAR IMPLANT

G. F. Harris, A. Sances, Jr., J. J. Ackmann, D. C. Hemmy, S. J. Larson and E. A. Millar*
The Medical College of Wisconsin, Milwaukee, WI and *The Shriners Hospital for Crippled Children, Chicago, Ill.

This report presents the findings in nine cases of cerebellar implant for cerebral palsy. Seven normal children with an average age of 9.75 years were also tested for comparison.

The biomechanical device utilized in these studies was built by Clinical Technology Corp. (Kansas City, Mo.) and delivered to the Department of Neurosurgery at the Medical College of Wisconsin in 1976. The device measures the passive resistance to motion of the subject's forearm through a force transducer mounted below the upper arm plate. This transducer is mounted in a manner which allows determination of tangential resisting forces to the circular path of motion. The displacement of the sensing arm is determined through the use of a potentiometer mounted at the junction of the sensing arm and lower support. A Chicago Nuclear X-Y recorder was utilized to obtain output hysteresis loops. The abscissa is in degrees of rotation and the ordinate is in units of torque about the elbow joint. A simple conversion process allows the abscissa to assume units of length and the ordinate to assume units of force. The work or energy required in passive motion is therefore an area measurement (Fig. 1).

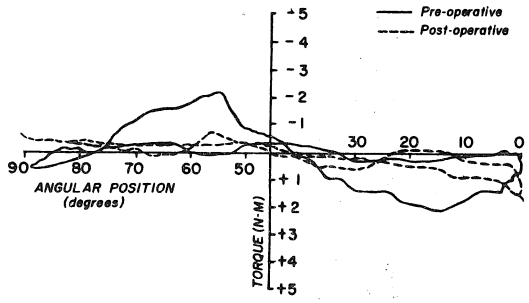

Figure 1

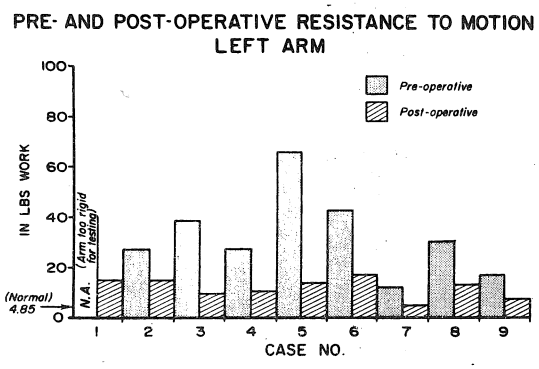

Figure 2

Testing of patients with cerebral palsy indicated a decrease in work after cerebellar implant for all nine cases tested in the left arm (Fig. 2). Eight of the nine subjects tested showed a decrease in work after implant in the right arm. One case indicated a slight decrease (Fig. 3).

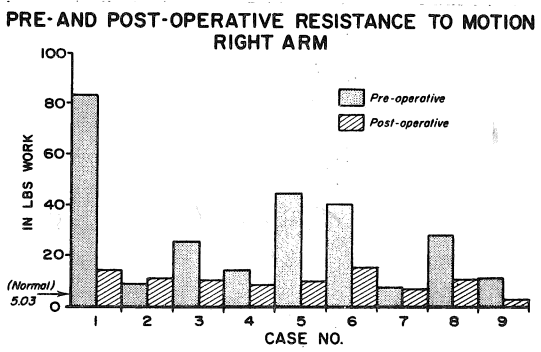

Figure 3

The Student's t test of operative findings indicates that the hypothesis that post-op resistance is less than pre-op resistance can be accepted with a confidence level of 99% (t=-3.502). This same hypothesis can be accepted for the right arm with a confidence level of 97.5% (t=-2.36) over the null that post-op = pre-op. The quantification of resistance in terms of work correlates as well with clinical findings. Thus further use of this and other devices which quantify resistance in terms of energy is being pursued.

Mailing Address: Dept. of Neurosurgery, The Medical College of Wisconsin, 8700 West Wisconsin Ave., Milwaukee, Wisconsin 53226

REMODELLING OF THE FEMUR MIDSHAFT IN AGING MALES

R. Bruce Martin
Division of Orthopedic Surgery
West Virginia University
Morgantown, WV 26506

A series of bone sections from 50 white male subjects, age 37 to 96, is being studied to elucidate the remodelling patterns associated with aging in men. Analysis of sections from the femur midshaft indicates that, while cortical area decreases with advancing age, porosity and the polar moment of inertia increase in a compensatory way. These results confirm previous reports and serve as a foundation for additional studies related to how and why these phenomena occur. These include to date measurements of osteonal and Haversian canal size and the number and distribution of canals in the various quadrants of the femur midshaft. These data indicate that osteons do not tend to change their overall (cement line) diameter with age, but that both the population and size of Haversian canals increase with age. The distribution of Haversian canals around the shaft shows age-related patterns which may be biomechanically induced. Also, histograms of the number of canals in a histologic field of view provide a mechanism for studying the manner in which osteonal remodelling is initiated and controlled. Using models of various remodelling schemes, the data are shown to be most consistent with remodelling which includes both random and controlled elements.

The importance of individual variations is discussed, along with the relationship of this work to previous studies and the general problem of skeletal aging.

AGE-RELATED CHANGES IN THE TENSILE STRENGTH OF CORTICAL BONE - A COMPARISON OF FOUR STUDIES

J. C. Wall
Department of Human Kinetics
University of Guelph
Guelph, Ontario
N1G 2W1

This paper compares the results of four studies which have attempted to demonstrate how the mechanical properties of human cortical bone change with age. The studies considered are Lindahl and Lindgren (1967), Yamada (1970), Burstein *et al.* (1976) and Wall. The results from these studies are summarized in the graph below.

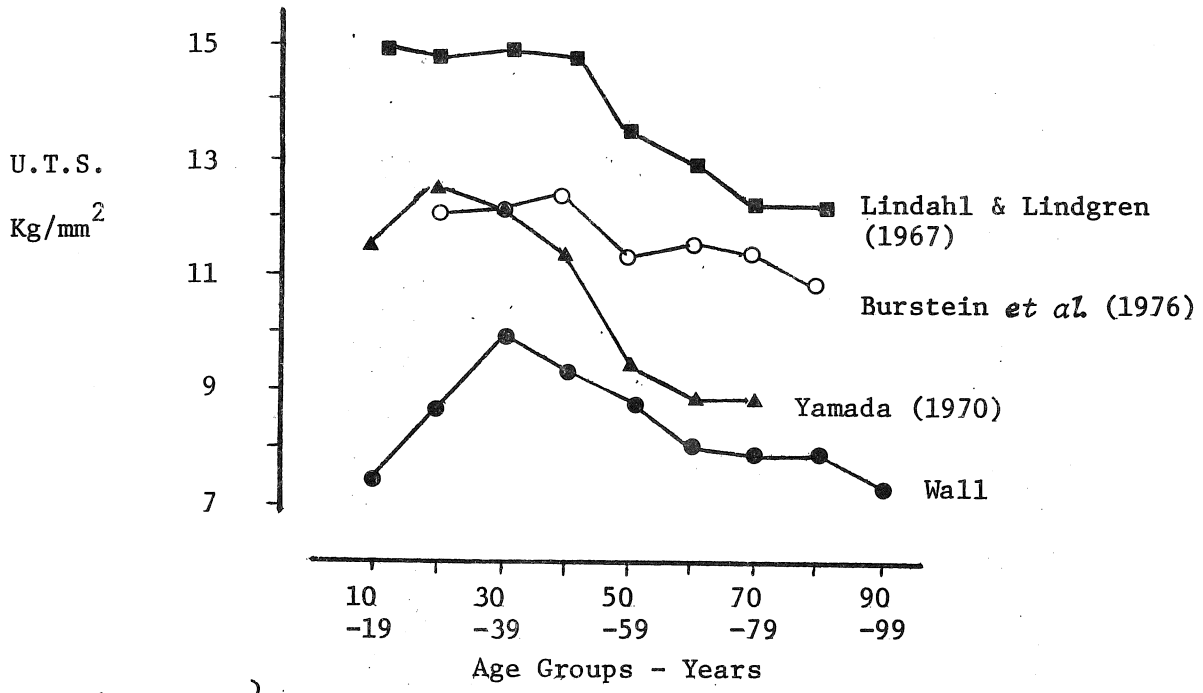

The common feature of these four studies is that there is a decrease in Ultimate Tensile Stress (U.T.S.) after the third or fourth decade of life. The Lindahl results, together with those of Burstein differ from the other two studies in that there is no peak, simply a gradual decrease in strength up to the fifth decade of life and thereafter a more noticeable decrease.

Although the trends shown by the four studies are similar the values of U.T.S. differ widely. Some possible causes for these differences are discussed to highlight the problems inherent in testing the mechanical properties of cortical bone and the equally important problems of interpreting the results of such tests.

REFERENCES

BURSTEIN, A.H., REILLY, D.T. and MARKENS, M.: Aging of bone tissue: Mechanical Properties. J. Bone Jt. Surg. 58A: 82-86 (1976).

LINDAHL, O. and LINDGREN, A.G.H.: Cortical bone in man. II Variation in tensile strength with age and sex. Acta Orthop. Scandinav. 38: 141-147 (1967).

YAMADA, H.: Strength of Biological Materials. Edited by F.G. Evans. The Williams and Wilkins Co., Baltimore, U.S.A. (1970).

IMPROVING HUMAN CONTROL OF TORQUE APPLIED TO BONE SCREWS

J. Cordey and S.M. Perren, Laboratory for Experimental Surgery,
Swiss Research Institute, CH-7270 Davos, Switzerland.

The efficiency of a bone screw in internal fixation is related to its axial tension which produces compression of the fracture surfaces. To permit functional treatment of a fracture, in is desirable to achieve optimal force (highest amount without failure of bone or screw). To limit the axial force, torque control is important. Can we improve human torque control in adapting to widely varying bone strength ?

30 experienced surgeons inserted 90 cortical screws (ASIF 4.5 mm) into 15 thawed human tibiae. The bones were grouped according to radiological density into 3 groups. An instrumented screwdriver and a resistive goniometer served to record torque (M) and angular displacement (α). Every surgeon placed a screw into one bone of each group. The surgeons were told to insert and tighten the screws applying an "optimal" amount of torque (M_{opt}); the torque was then increased untill stripping occured (M_{max}). M_{opt} was compared to M_{max}. The relationship between applied torque and rotation ($dM/d\alpha$) measured at the beginning of the tightening was compared with the maximum torque (M_{max}) and the stripping angle (α_{max}).

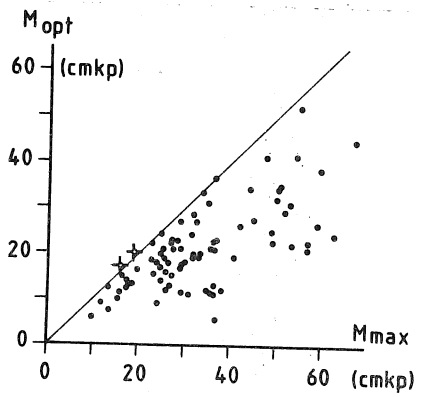

Fig. 1. Relationship between M_{opt} and M_{max}.

From the 90 measurements, 8 had to be rejected due to several unrelated reasons. The relationship between M_{opt} and M_{max} is given in figure 1. Unexpected stripping occured at low amount of torque (+).

	Mean ± $S_{\bar{x}}$	Min. - Max.	
$dM/d\alpha$	24.9 ± 2.74	(18.3 - 164.0)	cmkp/2π
α_{max}	0.79 ± 0.021	(0.39 - 1.43)	2π
M_{max}	33.3 ± 1.46	(10.0 - 66.8)	cmkp

(10 cmkp = 0.981 N.m)

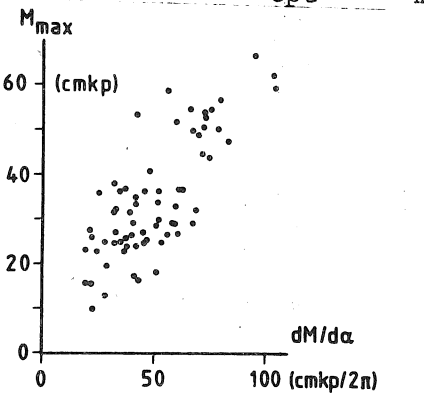

Fig. 2. Relationship between M_{max} and $dM/d\alpha$.

The comparison of $dM/d\alpha$ and M_{max} shows a significant correlation (Spearmann $R = 0.65$; $p < 0.001$, figure 2) in the same way as $dM/d\alpha$ and α_{max} ($R = 0.44$; $p < 0.001$); the correlation between M_{max} and α_{max} is less strong ($R = 0.23$; $0.02 < p < 0.05$).

The feeling of the surgeon, probably based on $dM/d\alpha$, has been shown earlier to be superior to the help offered by torque limiting devices with preset torque level. In porotic bones however the feeling has some shortcoming. It will be shown how the relationship between $dM/d\alpha$ and M_{max} may be used to supplement the feeling in order to prevent unexpected stripping.

A SIMPLE IN-VIVO BIOMECHANICAL KNEE STABILITY TEST

Torzilli, P.A., Greenberg, R.L., Insall, J.N. and Marshall, J.L.

The Biomechanics Dept., The Hospital for Special Surgery, New York, N.Y.

INTRODUCTION: Clinical evaluation of knee stability provides a qualitative measure of the amount of relative motion between the femur and tibia. Various types of mechanical apparatus exist for performing knee stability tests. These objective machines usually employ either a hydraulic load/radiographic measurement arrangement, or a uniaxial load/displacement transducer instrumented exoskeleton. Both these devices are mechanically complex and can possess certain inherent inaccuracies. In the former, patient motion can cause load variations, while both displacement techniques are of limited accuracy as they do not account for the effects of out-of-plane motions. Therefore the objectives of this investigation were to (1) develop a simple stress machine for the application of a constant static load, (2) evaluate radiographic measurement technique which would account for out-of-plane motions, (3) determine the amount of relative femoral-tibial motion in a stable population, and (4) construct a methodology for the evaluation of the clinically unstable knee.

METHODOLOGY: A simple test machine was constructed utilizing a height adjustable seat, a restraining foot cup, an adjustable x-ray cassette holder and height adjustable, constant tension springs, all affixed to a movable platform. The patient's foot was fixed in the restraining cup and the seat adjusted to obtain a 90 degree flexion angle. The patient's leg was relaxed with the cassette held on the medial aspect. For loaded testing a cuff was placed at mid-calf and the spring attached such that either an anterior or posterior force was applied. Loaded and unloaded radiographs were made bilaterally.

To evaluate a radiographic measurement technique cadaver knees were placed in jigs and positioned to duplicate the unloaded 90 degree flexion configuration. All ligamentous constraints were sectioned and out-of-plane motions, consisting of femoral ab/adduction, tibial rotation, and femoral rotation were imposed. Lateral radiographs were taken at incremental angular changes and the measured distances shown below recorded. These were used in a multiple linear regression in order to obtain corrections for out-of-plane motions.

RESULTS: Twenty-two ligament stable patients were evaluated using 15 and 30 pounds of force. Mean total tibial A-P displacement did not differ statistically between opposite limbs for the sample population. Similar results were found for anterior and posterior displacement and for the neutral position, defined to be the relative position of the tibia and femur in the unloaded state. Mean tibial displacements are shown below. Utilizing the mean displacement, the difference between contralateral sides, and the neutral position a methodology for the statistical evaluation of the unstable knee was formulated.

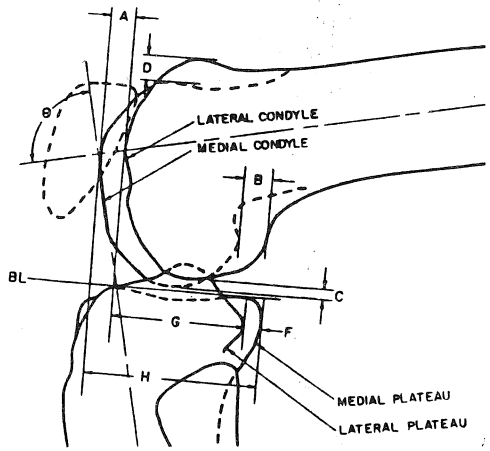

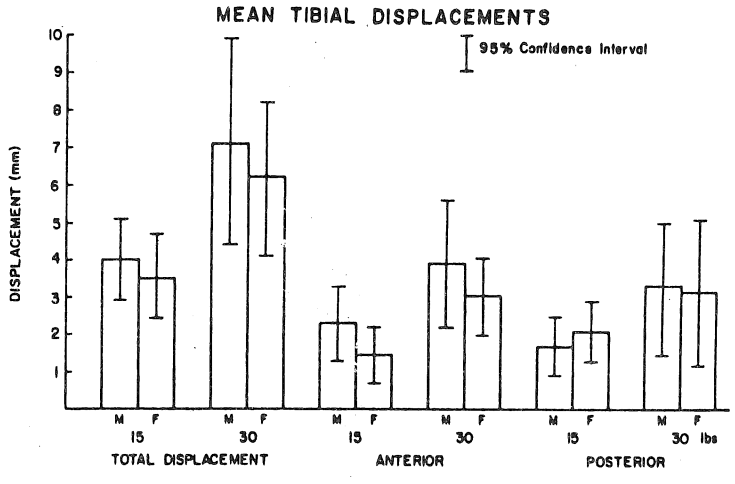

STRENGTH OF PATELLAR TENDON REPAIR IN RABBITS

J. David Blaha, M.D., Larry S. Matthews, M.D. and
David A. Sonstegard, Ph. D.*

The timing of rehabilitation and the vigor with which it is carried out following repair of ligament or tendon should depend largely on the strengh of the healed structures. Three general types of repairs have been used by surgeons: Simple tendon to tendon suture (Type I) is easily accomplished but said to be weak and subject to stretching under load. Tendon sewn onto exposed cortical bone (Type II) is thought to provide a stronger healed unit. Tendon anchored through the cortex into trabecular bone (Type III) is reputed to be superior in strength and worth the technically difficult operation required.

To adequately plan operative therapy and rehabilitation for ligament and tendon repair, the ultimate tensile strength of each type of repair was determined at six and twelve weeks following operation on the patellar tendon of rabbits. For each rabbit one hind limb was used for operation, the other for control. The results would seem to indicate the following:

1. All repairs (i.e. Type I, II and III) are significantly weaker than controls at six weeks - roughly 1/2 the tensile strength.

2. Tendon to tendon (Type I) repairs are statistically indistinguishable from controls at twelve weeks.

3. Both tendon to bone (Type II) and tendon into bone (Type III) repairs are significantly weaker than controls at twelve weeks, although they had gained considerable strength, to a value roughly 75% of the control strength.

*Section of Orthopaedic Surgery, University of Michigan Medical Center, Ann Arbor, Michigan

Biomechanical Aspects of the Bicep Tendon Transfer

Branham, R., Clancy, W.G., Jr., Narechania, R.G.

Introduction

The biceps tendon transfer is an intergral part of a combined procedure to correct knee instability. This portion of the operative procedure is a dynamic correction for anterolateral instability and the anterior subluxation of the tibia on the femur. This investigation attempts to construct a biomechanical model of the tendon transfer that aids in dynamic stabilization of the knee. The procedure can be briefly stated as the one in which the biceps tendon of the long head is removed from its insertion on the fibula head and passed beneath the fibula collateral ligament and re-inserted distally at the level of gerdeys tubercle such that the portion of the fibular collateral ligament attachment at the femur now acts as a pulley.

Model

Before the surgery the force vectors were acting more in the superior direction as shown in figure 1. It has a small component ($\overline{LH}$) that also produces a force in the lateral direction.

After the surgery, due to the change in insertion position the resultant force is acting more in postero-lateral direction ($\overline{FG}$) as shown in figure 2 ; point B is the fibular ligament point below which the tendon is passed and is acting as a pulley. The vector diagram also shows a larger component ($\overline{LG}$) now acting laterally - preventing the anterior-lateral instability; and a component acting a little more posteriorly ($\overline{BG}$) that would eliminate the anterior subluxation of the tibia. Consequently a planted internally rotated foot will not subluxate anteriorly when the knee is flexed.

Summary

A biomechanical model of the biceps tendon is described. Due to the new insertion position of the tendon, the resting length of the muscle increases. This enables the muscle to act as a stronger external rotator and adds a component in the posterior direction that prevents anterior subluxation.

Figure 1

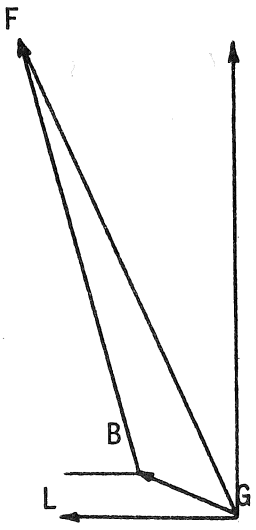

Figure 2

For information address to
Rajesh G. Narechania
University of Wisconsin
Orthopedic Surgery
Madison, Wi 53706

COMPRESSIVE STRENGTH OF SOME CARIBBEAN CORALS

John A. Chamberlain, Jr. & Arthur Shapiro

Department of Geology
Brooklyn College of the
City University of New York
Brooklyn, N.Y. 11210

One of the primary functions of the skeleton of corals is to support the tissues. As in other skeletonized groups, the mechanical properties of coral skeleton should be of major adaptive significance because they influence such factors as maximum colony size, and the range of hydraulic conditions a colony can withstand without breakage. In order to evaluate these ideas, we have examined compressive strength and elastic modulus of three common Caribbean corals: Acropora palmata; Montastrea annularis; and Siderastrea radians.

Specimens prepared from material collected in Jamaica, Florida, and St. Croix were tested in a Donath triaxial deformation apparatus. Results of these tests indicate: (1) coral skeleton develops fractures similar to those of mechanically anisotropic rocks like slate. In the case of corals, anisotropy results from the growth direction of the polyps. (2) coral skeleton exhibits linear stress/strain curves and fractures at strains of about 0.3%. It is thus a brittle material, and in this respect is similar to the skeletons of many other types of organisms. (3) compressive strength for these corals is 12-81 MNm^{-2} (mean = 48 MNm^{-2}). This is lower than the strength of mammal bone and mollusc shell, but higher than that of carbonate engineering materials. (4) the relatively low strength of coral skeleton is due to its high porosity and its lack of a significant organic matrix, and may reflect limitations on strength due to competing adaptive needs or low probability of breakage before attainment of reproductive parity. (5) as a result of alignment of septa and thecal walls, coral skeleton is stronger when stress is applied parallel to the growth direction of the polyps than when applied perpendicularly. (6) strength decreases as porosity increases. This decrease follows Ryskewitch's rule for ceramics. (7) porosity increase produced by even relatively minor boring of the skeleton can reduce strength by about 50%. (8) corals like A. palmata that have small polyps and low porosity are stronger than those like M. annularis that have large polyps and higher porosity. This observation suggests that the skeleton of branched growth forms is stronger than that of massive growth forms. (9) skeletal strength is comparable to the stresses produced by many relatively common hydraulic events. This suggests that some corals may need specialized geometric adaptations to survive in some reef locales. (10) strength of A. palmata is correlated with habitat. Strong, low porosity skeletons occur in highly energetic locales (reef crest), while weaker, higher porosity skeletons are found in quiet water environments (backreef, forereef).

Our results suggest that material properties of the skeleton are important factors in the adaptive response of corals to physical conditions of their environment.

KINETICS OF FRACTURE HEALING OF MANDIBULAR BONE FOLLOWING SAGITTAL SPLIT OSTEOTOMY OF THE PORCINE MANDIBULAR RAMUS

Diane Margel Robertson and D. C. Smith, Faculty of Dentistry, Univ. of Toronto
Suman K. Das and I. Munro, Hospital for Sick Children. Toronto, Canada

Orofacial surgical techniques, which are concerned with repair of fractures, congenital defects and occlusal dysfunctions, frequently utilize sagittal osteotomy of the mandible to achieve desired clinical results. Currently, however, the period of immobilization following osteotomy in humans is arbitrary (generally 6-8 weeks). There is no scientific basis for the selection of this time period; further, there have been no studies which assess bone strength gain following the osteotomy. The primary purpose of the present study, then, was to determine the rate of return of the bone to its normal physical and mechanical properties following controlled surgical osteotomy and fracture treatment. This study follows a 2-year materials characterization study of normal porcine mandibular bone. The pig was utilized in view of its wide use as a surgical model and its ease of supply.

A reverse modified Obwegeser-DalPont sagittal osteotomy was performed. The proximal osteotomy was on the outer cortex, which ran horizontally and the distal osteotomy was on the inner cortex, which ran vertically. These osteotomies were joined by a sagittal osteotomy which ran along the free lower border of the body/angle and posterior free border of the ramus. Immobilization was carried out with 3 intra-osseous wires. The left side was operated on, leaving the right side to be used as a control. This preliminary study utilized 6 pigs, 2-3 months old (60-70 lb), so that the ramus was of adequate thickness (4-6 cm) to perform the osteotomy without fracturing the cortices. Healing times were 2, 3 and 4 weeks following surgery. A continuing study will utilize healing times up to 6 months.

The properties of each mandible were evaluated following sacrifice. Compressive, tensile and shear strength data were obtained from regions within the osteotomy site and congruous regions from the control side. Stresses do not attain normal values within this short time interval, but an increase in strength with time is noted and it is hoped that the final study will yield a healing rate equation. The x-ray transmittance of healing bone varies as bone remodelling and mineralization proceed. By densitometer measurement of radiograms, we followed the progress of healing and correlated the increase in x-ray opacity with mechanical observations. Microdensitometry appears to be a promising tool for the clinician. Several preliminary experiments involving the chemical analysis of the fracture interface were attempted by exploitation of Auger electrons from a thin surface layer of this interface. These measurements were carried out at the same time as scanning electron microscopy to locate and identify the feature on the fracture surface which was being analyzed. We have been able to detect increasing calcium content with time in the osteotomy region and healing callus and it is hoped that this will prove an effective physical means of monitoring mineralization kinetics. Since bone labels deposit themselves <u>in vivo</u> in sites of bone formation, they can be studied in undecalcified sections by fluorescence microscopy. The labels are time markers with which one can microscopically measure bone formation kinetics. Rate information can be obtained by measuring some change (e.g. x-ray opacity) which has taken place between two successive moments in time (2 successive labels). This analysis is currently underway.

Supported by a grant from the Hospital for Sick Children Foundation and the Canadian Fund for Dental Education.

AN EXPERIMENTAL INVESTIGATION OF THE EFFECTS OF REPETITIVE STRESS ON LIVING CANINE BONE

Susan Schein
R. Bruce Martin
Division of Orthopedic Surgery
West Virginia University
Morgantown, WV 26506

The human skeleton is a structural framework which has the ability to detect and repair microdamage that results from repetitive stress. When an increase in the normal level of stress is allowed to continue without adequate rest, the microdamage accumulates faster than it can be repaired. The result of this situation is a fatigue response to fracture in the bone depending on the magnitude, frequency and duration of the stress applied. Numerus in vitro experiments have been conducted to determine the fatigue behavior of compact bone specimens. In order to gain a better understanding of the fatigue process as it occurs in vivo, the present study was designed to examine the effects of repetitive impact loading on the compressive strength, stiffness and remodelling of living canine bone. The dogs used in this study came from two mongrel litters. Each dog was kept in an activity-limiting cage from birth to the end of the experiment. At age 17 weeks repetitive loading was begun on 4 dogs. This procedure involved lifting the dogs 1 m. off the floor and then releasing them to land on all four limbs. The number of load cycles averaged 500 drops/day for 2 dogs (litter 1) and 1000 drops/day for 2 dogs (litter 2). Total number of weeks treated was 4,5, or 6. Three control dogs (1 from litter 1, 2 from litter 2) remained in the activity-limiting cages without being dropped for 5 weeks. Tetracycline was administered 5 days before sacrifice. No fatigue fractures were observed by roentgenographic or histologic analysis. A 1 cm. section from the distal shafts of the left tibia, femur, humerus, and ulna of each dog was used for a compression test. Based on the normalized (by body wt.) values for each bone tested, it was found that the bones of the treated dogs were stronger and stiffer than the control dogs. Based on the presence of the tetracycline label, there was a noticeable yet statistically insignificant increase in the combined periosteal and endosteal remodelling for the femurs in the treated dogs. No such difference existed in the tibias. There appeared to be no discernable pattern nor significant difference in the cross-sectional area, number of resorption spaces, labelled osteons or porosity of the treated and control groups. Failure to produce a fatigue response or fracture in the bones is best explained by the hypothesis that the level of repetitive stress applied was insufficient to exceed or alter the already extremely active remodelling process of an immature skeleton; and instead seemed to serve as a stimulus for improved bone strength.

Ground Reaction Forces in Human Locomotion

by Peter R. Cavanagh, Biomechanics Laboratory

Pennsylvania State University, University Park, Pennsylvania 16802

The study of ground reaction forces during human locomotion has been a major area of Biomechanics research since the beginning of the twentieth century.

This paper aims first to provide a comprehensive survey of the measurement techniques used. This survey begins with the ingeneous attempts of early investigators like Amar (1923), Basler (1927), and Elftman (1934), and concludes with the more recent innovations of Arcan and Brull(1976), Nicol and Henning (1976), and Deibschlag (1977). This review shows a diversity of techniques available to measure the ground reaction forces and the resulting pressure distributions. However, the knowledge gained from previous experiments provides remarkably little return on the heavy investment of instrumentation.

A review of the literature pertaining to ground reaction forces during normal and abnormal walking and running forms the basis of the second part of this paper. The use of force and center of pressure data from a force platform is discussed as it relates to footwear design, classification, diagnosis and treatment of gait abnormalities and mathematical modelling of the lower extremity. The need for more comprehensive data on the pressure distribution beneath the foot is addressed and examples of distributions obtained during static and dynamic activities are presented.

References:

1. Arcan M., and M.A. Brull. A fundamental characteristic of the human body and foot, the foot-ground pressure pattern. J. Biomechanics. 9: 453-457, 1976.
2. Amar, J., Le Moteur Humain. Dunod, Paris, 1923.
3. Basler, A. Bestimmung des auf die einzelnen Sohlenbezirke wirkenden Teilgewichtes des menschlichen Körpers. Abderhalden's Handbuch, Abt. V. Teil 5A, Heft 3, S 559-574, 1927.
4. Diebschlag, V.W., W. Müller-Limmroth, H.R. Bierlein. Die Komponenten der resultierenden Kraft unter der Fusssohle des Menschen beim Gehen. Das Leder. 28: 202-209, 1977.
5. Elftman, H. A cinematic study of the distribution of pressure in the human foot. Anatomical Record. 59(4): 481-491, 1934.
6. Nicol, K., and E.M. Hennig. Time-dependent method for measuring force distribution using a flexible mat as a capacitor. In: Paavo V. Komi (ed.), Biomechanics V-B, 433-440, 1976.

TITLE: Analysis of the Developmental Changes of the Running Patterns of Female Children

AUTHORS: Eugene W. Brown, California State University, Los Angeles; and Barry T. Bates, University of Oregon, Eugene

This explorative cross sectional study investigated the developmental characteristics of the running patterns of skilled preschool, kindergarten, second, and fourth grade girls. They were selected on the basis of a time criterion on the 30 yard dash. Two principle questions were investigated: 1) Is it possible to evaluate developmental trends and traits on the basis of temporal and kinematic quantities describing the body and body segments? 2) Can developmental changes occuring in the running patterns of children be differentiated using Fourier (harmonic) analysis of the paths of selected body landmarks?

One complete running stride of each subject was filmed and analyzed. Time and position data describing the paths of the right ankle, knee, hip, and shoulder joints were obtained from film. The stride was divided into 21 different intervals (phases). Subject groups were compared using analysis of variance of the absolute and relative times for completion of these intervals. The kinematic analysis consisted of analysis of variance between groups on stride length and velocity using both actual and standardized subject heights. Additionally, total body and body segment positions were compared using analysis of variance for 11 different positions. The Fourier analysis consisted of a comparison of the harmonic coefficients of the horizontal and vertical motions of selected joint centers with respect to time.

Based upon the analyses, the following results were drawn: 1) There was an indirect relationship between grade level (age) and the absolute time required to complete the interval mid-support to the last frame of contact for both feet. 2) The support phase generally exhibited a decreasing absolute and proportional time trend with increasing age. 3) The preschool children demonstrated significantly shorter time and smaller proportion in the second nonsupport phase. 4) Actual stride lengths increased significantly with age. 5) There was a direct relationship between mean stride velocity and age. Actual velocity increases were not entirely the result of increased subject height. 6) At right foot strike, the preschool children positioned their bodies farther behind their ankle joints than did the older children. 7) At take-off from the right foot, the preschool children exhibited a significantly greater hip joint extension. 8) During the last frame of the contact with the left foot, the orientation of the right side of the body of the preschool children significantly differed from the other groups. 9) During the last frame of right forward swing, the older children tended to have their thigh held higher with respect to their trunk and their foot held closer to their buttock. 10) The first harmonic contributed the greatest percentage to the reconstruction of the horizontal motion of all joint centers for all grade levels. 11) The first harmonic contributed the greatest percentage to the reconstruction of the vertical motion of the ankle joint for all grade levels. 12) The second harmonic contributed the greatest percentage to the reconstruction of the vertical component of the motion of the hip and shoulder joints for all grade levels. 13) Trends in the harmonic reconstruction of the horizontal joint center movements were not evidenced except in the hip joint, where the second harmonic was relatively more important in the older and faster subject groups. 14) Trends in the harmonic reconstruction of the vertical joint center movements were evidenced in the knee, hip, and shoulder joints. There generally existed a direct relationship between grade level and the mean relative magnitude of the first harmonic. These relationships were reversed in the second harmonic. This finding supported the conclusion that skillful runners have a smoother and less erratic vertical movement.

THE EFFECT OF RUNNING SPEED ON FOOT-TO-GROUND FORCES

Richard M. Harrington and Frederick G. Lippert, III, M.D.
Biomechanics Research
Veterans Administration Hospital
4435 Beacon Avenue South
Seattle, Washington 98108

Variations in running speed produce many changes in body kinematics and kinetics. Stride length, stride frequency, flexion-extension of the ankle, knee and hip, and foot-to-ground forces are all effected. The purpose of this research is to study the variation in foot-to-ground forces of several subjects while running at a range of speeds.

The system for measuring the forces and moments acting between the ground and the shoe worn by the subject consists of two dynamometers attached at the toe and heel of a running shoe. Forces and moments cause deflections in a machined aluminum cross to which 8 strain gauge half-bridges are attached. The analog voltage signals from the strain gauges are digitized and stored on cassette tape in the data collection system carried by the subject in a backpack. Each cassette can record 10 minutes of data, allowing for multiple strides to be sampled at each running speed. The cassettes are read into a computer for processing into force and moment components resolved about three mutually orthogonal axes. At least 10 strides are recorded at each running speed to allow for average values of force and moment components to be calculated.

Running is growing rapidly in popularity as a means to attaining and maintaining cardiovascular fitness. Unfortunately for many runners as their condition improves and they increase the amount or speed of their running, they begin to experience overuse problems in their lower limbs and back. Shoe design, stretching and strengthening exercises, and proper training schedules are factors which contribute to an individual's ability to run more. The information provided by this research should benefit shoe designers, sports medicine physicians, coaches and runners.

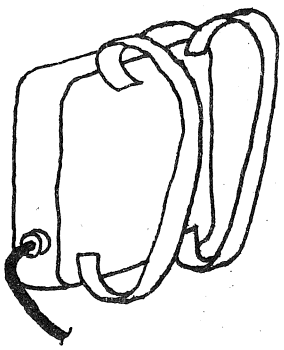

Data Collection System

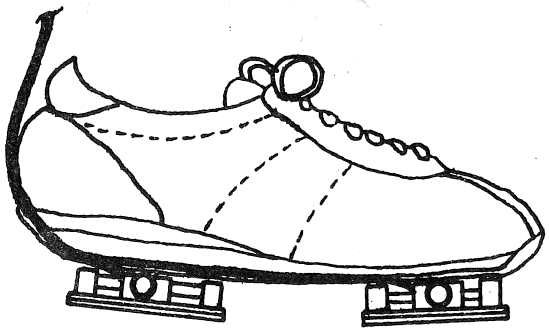

Toe & Heel Transducers

EFFECT OF RUNNING SHOES ON SELECTED ASPECTS OF LOWER EXTREMITY FUNCTION.

B.T. Bates, S.L. James, L.R. Osternig and B.R. Mason, Biomechanics/Sports Medicine Lab., University of Oregon, Eugene, OR

In recent years, extensive shoe evaluations have been made in attempts to objectively examine the various shoes available to running enthusiasts. This has resulted in an increased awareness by shoe consumers and manufacturers as to some of the important characteristics of a good running shoe. The purpose of this project was to examine the dynamic effects of different running shoes on selected aspects of lower extremity function during the support phase of running. Two subjects were filmed during controlled overground running utilizing two cameras operating at 200 frames/sec. Films were obtained of the foot and lower leg for three trials each of five test conditions. Film analysis was performed using stop action projection with a digitizer interfaced to a 4051 Tektronix Graphic System. All data were treated mathematically with a cubic spline function to minimize measurement error and allow for multiple trials to be averaged. This provided a more accurate representation of the effects of each condition on lower extremity function. The mean values of maximum pronation resulting from the five test conditions ranged from 6.2 to 11.6 and 7.6 to 15.8 degrees for each subject, respectively. In addition to the primary maximum value which occurred relatively early in the support phase (20-30%), most conditions also produced a secondary peak value of lesser magnitude later in the support period (50-60%). These peaks appeared to be the result of changes in leg rather than heel orientation. Examination of the shoes suggested that the amount of pronation was influenced by such factors as relative heel height, firmness of heel cushion, and heel counter construction and fit. A shoe's ability to absorb shock at impact was judged on the basis of the vertical displacement of the malleoli during the initial phase of the support period. Some shoes were observed to have a relatively quick rebounding effect on the ankle joint, followed by a second compressive phase. The different shoes produced modified lower extremity function and a shoe's potential to control pronation and absorb shock appeared to be inversely related functions.

IN VIVO MEASUREMENT AND ANALYSIS OF BONE STRAIN

D.J. Smith*, D.R. Carter, D.M. Spengler, and V.H. Frankel
Department of Orthopaedics and Center for Bioengineering
University of Washington Seattle, WA 98195

The strains and stresses experienced by bone tissue in vivo are of major clinical concern. A better knowledge of in vivo bone loading may lead to improved techniques of internal fracture fixation and joint replacement. In addition, assessment of bone strain and stress fields will provide a better understanding of clinical disorders such as fatigue fracture, pathological fracture, and the stress-related remodeling response of bone. Most previous attempts to estimate in vivo stresses have relied on theoretical methods based on simplifications of the anatomy and material characteristics. The complex geometry and loading conditions of bone in vivo limit the accuracy and usefulness of these theoretical analyses. Strain gages bonded to the bone surface provide the most direct and reliable measure of in vivo strains under physiological conditions. A strain rosette (composed of three single gages oriented at different angles) is required to completely define the state of strain on a surface simultaneously subjected to longitudinal, transverse, and shear stresses.

In this study, an in vivo technique of bonding strain rosettes on canine radii and ulnae was developed which allowed continuous strain measurements during gait. An integral unit of insulated rosette gage, lead wires, flange, and multiple pin connector (plug) was prepared for each experimental animal. A stacked rosette with an active gage length of 1.6 mm was employed. The temperature effects were minimized by use of a low-excitation voltage of one volt DC. The fine wires (0.13 mm) from the gage were soldered to small conductor tabs arranged circumferentially around the gage. To these tabs, larger ultraflexible copper conductor Teflon-coated leadwires were attached. The plug was tunneled subcutaneously to the upper thoracic region, delivered through the skin, and connected to a multichannel recorder. The dog was placed in a jacket, and the plug was secured in the jacket pocket when rosette recordings were not being made.

Daily recordings were made for each animal during normal gait on a tile floor. An assistant walked the animal on a leash while holding the cable. Two to three days after gage application most animals had a normal gait. The position and orientation of each rosette on the bone were established by radiography and later confirmed by postmortem examination. The animal's gait velocity was approximated by measuring the time elapsed in completing an eight-meter course. Data analysis consisted of calculating the strains and stresses in the principal material directions (long bone axis system). The stress calculations were made using an anisotropic technique (Carter, in press) which incorporates the elastic constants of cortical bone as determined by Reilly and Burstein (1975). The results showed that significant longitudinal, transverse, and shear stresses were present on both the radius and ulna rosette sites during normal gait. These findings suggest that the in vivo loading conditions are complex and that the interosseous membrane transmits considerable forces during normal gait.

We thank Richard Lee and Vivian Johnson for technical assistance.

Carter, D.R. (In press) J. Biomech.
Reilly, D.T., and Burstein, A.H. (1975) J. Biomech. 8:393-405.

*Current Address: Department of Orthopaedics, Loyola University, Maywood Illinois 60153

BONE STRENGTH, MINERAL CONTENT, AND RESONANT FREQUENCY

J. M. JURIST and R. K. SNIDER, Saint Vincent Hospital, Billings, Montana, and Montana State University, Bozeman, Montana

This study determined the degree to which fresh bone breaking strength could be estimated from potentially noninvasive measures of skeletal status and tested the validity of a simple model used to relate bone resonant frequency to mineral content and geometry.

One hundred twelve humeri were excised from 57 New Zealand white rabbits weighing 1-2 Kg and kept wet before and during testing. Midshaft mineral content was measured with the bones submerged in normal saline by the 125-I photon absorptiometric method. Midshaft width (in the anteroposterior direction) and length was measured with a vernier caliper. First flexural resonant frequency was measured with the bone ends free by means of a B&K Type 8000 mechanical impedance transducer attached to a B&K Type 4810 minishaker. The resonant frequency was that frequency for which driving point mechanical impedance was at a minimum. A load deflection curve was determined for each bone in a modified Comten Industries materials testing apparatus in 3 point bending with the anterior side under tension (5 cm span, deflection rate of 10 cm/min). Breaking strength was obtained directly from the load deflection curve, and the average bending stiffness between 10-50% of the failure load was also determined.

Both resonant frequency and mineral content were significantly correlated with bone strength ($r=0.48$ and 0.75, respectively). The stepwise multiple regression of strength on resonant frequency and length yielded a multiple correlation coefficient of 0.81.

An analytical model for the humerus was derived in which it was assumed to be a uniform hollow cylinder composed of homogeneous isotropic material which behaves linearly up to the failure point, and which fails at a constant strain. The cylinder is filled with soft tissue of negligible Young's modulus to simulate the mass loading effects of marrow. The bone ends are assumed to be free as they were during the resonant frequency determinations.

A linear association was found between observed bending stiffness and flexural rigidity calculated on the basis of the model ($r=0.77$). A correlation coefficient of 0.80 was found between measured bone breaking strength and that predicted on the basis of the model. This correlation coefficient is essentially identical to that obtained from the stepwise multiple regression of strength against the same parameters used in the model ($r=0.81$), thus showing that the model yields results as good as can be expected for the available data.

These findings suggest that the analytical model is sufficient for use in predicting bone breaking strength based on the noninvasive measures of flexural resonant frequency, midshaft mineral content and width, and length. In addition, the highly significant association between actual breaking strength and that calculated on the basis of the model accounts for about 65% of the variance in observed strength.

ACKNOWLEDGEMENT: This research was supported by NIH Grants AM-16514, AM-17804, and AM-20130.

Elastic and anelastic deformation in compact bone

W. Bonfield, M.D. Grynpas[+], P. O'Connor*

Department of Materials, Queen Mary College, University of London, London. E1 4NS, U.K.

The elastic and non-elastic deformation characteristics of compact bone specimens have been determined with ultrasonic and microstrain techniques. It was found that the variation of Young's modulus of bovine femur specimens with the orientation of the specimen axis to the long axis of the bone did not follow the theoretical predictions of a fibre reinforced composite model.

Measurements of the tensile stress-strain behaviour of longitudinal bovine and rabbit compact bone specimens, revealed a series of closed hysterisis loops, which are attributed entirely to anelastic deformation. The concept of a friction stress, which defines the onset of anelastic deformation, is introduced.

[+] Now at Childrens' Hospital Medical Center, Boston, Massachusetts, U.S.A.

* Now at Dept. of Pathology, University of Manchester, U.K.

MECHANICS OF RED BLOOD CELLS

Professor Richard Skalak
James Kip Finch Professor of Engineering Mechanics
Department of Civil Engineering and Engineering Mechanics
Columbia University
New York, N.Y. 10027

Information on the properties and behavior of red blood cells has been greatly expanded during the past decade. The behavior of red blood cells is important to blood rheology and the relative availability and simplicity of the red blood cell has made it possible to obtain more detailed experimental information and to perform analytical computations in greater detail than for most other cells of the body. The red blood cell may be modeled as a thin viscoelastic shell filled with a homogeneous incompressible viscous fluid. The membrane is isotropic with respect to directions in the plane of the membrane but being a distinctly layered structure two molecules thick, it is anisotropic in the normal direction. The arrangement of the lipid molecules which make up the bulk of the membrane is similar to a double layer of liquid crystal molecules. This has led some authors to develop a liquid crystal theory of red blood cell membranes. Such a theory includes a bending resistance of the membrane but no shearing elasticity. The red blood cell membrane does exhibit a distinct shear elasticity due to the fact that a substantial amount of protein mostly spectrin is closely associated with the inner surface of the membrane. The deformation of this associated protein network is probably the source of the viscoelasticity of the membrane in shear also. In any case even for very large deformations the surface area of the red blood cell remains nearly constant. Its modulus of elasticity in areal expansion has been measured as well as its dependence on temperature. The areal modulus is about four orders of magnitude greater than the shear modulus. The complete model described above appears to be capable of explaining a variety of observed behaviors of the red blood cell such as pipette experiments, unidirectional extension, sphering, shearing, tank treading and bulk viscoelasticity. It has also been used to model capillary blood flow realistically. With appropriate incorporation of molecular adhesive forces and fracture criteria, this model may also account for rouleau formation and the hemolysis of red blood cells under various conditions.

BIOMECHANICS OF TRACHEAL CLEARANCE *

Anthony T. W. Cheung
Department of Biology
Loyola Marymount University
Los Angeles, California 90045

Tracheal mucus transport represents the only means of clearance in mammalian respiratory tracts against hazardous foreign particles, liquid-droplets, cellular debris and harmful bacteria. Transport (clearance) is mucus-dependent, muco-ciliary in nature and is achieved through a continuous escalation of the mucus blanket of the tracheal muco-ciliary system in a conveyor-belt manner.

The unique beat characteristics of tracheal cilia (which differ significantly from all types of micro-organism ciliary pattern), the effective uni-directional ciliary currents caused by the unique forward strokes, the muco-ciliary interactions, the loading-unloading characteristics of tracheal mucus, the particulate transport rate of the mucus blanket and its functional characteristics have been quantitatively investigated.

A model has been adopted for predicting the mucus transport (clearance) rate of the muco-ciliary system ------ the mechanics of such a model is based on the conveyor-belt mechanism as described quantitatively by Cheung and Jahn (1975, 1976) and Cheung and Chwang (1978). The cilia, in their normal beat cycles, have a periodic penetration contact with the bottom of the overlying mucus blanket during the early stage of the planar forward strokes. The unique bent (resting) configuration of the tracheal cilia, the effective uni-directional movement of the surrounding fluid (ciliary currents) and the mucus-fluid interaction all help to contribute to the overall mucus transport. The predicted average mucus transport rate is found to depend linearly on the beat frequency of the tracheal cilia and also on the contact time between the tips of the cilia and the bottom of the mucus layer. Such theoretical predictions are in good agreement with experimental observations.

The tracheal muco-ciliary clearance system will also be discussed with reference to the biochemical and rheological properties of mucus and the beat characteristics of tracheal cilia. The functional characteristics of such a muco-ciliary system will be examined with especial emphasis on tracheal clearance in normal physiological conditions as well as on the absence of clearance in pathological conditions.

* A 16mm high-speed movie will be shown with the presentation.

HYSTERESIS OF WHOLE BLOOD, A VISCOELASTIC EFFECT

Samuel E. Moskowitz
The Hebrew University, Graduate School of Applied Science and Technology, Division of Applied Mathematics, Jerusalem, Israel.

It is well known that whole blood is a non-Newtonian incompressible fluid: its apparent shear viscosity, in the Poiseuille sense, is a function of erythrocyte concentration and shearing strain rate. In particular, the rheological behavior at low rates is time dependent, a property usually referred to as thixotropy. Dintenfass (1) obtained a hysteresis loop when he determined blood viscosity at varying rates between 1.7 and 0.05 sec^{-1} on 18 normal subjects using the rhombospheroid viscometer at 37°C. Apparent viscosity was measured first at decreasing rates of shear, then, immediately thereafter, at increasing rates.

This investigation was undertaken to determine whether the aforementioned experimental results were a natural consequence of a viscoelastic response to a reversal of loading direction in simple shear flow.

Two viscosities (λ_0, λ_1) were considered at every point in a general flow field: coefficients of principal strain and maximum shearing strain rates, respectively, in the constitutive relation

$$\tau_{ij} = \mu e_{ij}$$

where

$$\mu = \begin{cases} \lambda_0, & i=j \\ \lambda_1, & i \neq j \end{cases}$$

The viscosities were related by

$$\lambda_1 = \lambda_0 (1+\chi)^2$$

$$\chi = \eta(C) |e_{ij}(x)|^{-n} / 2\lambda_0(C), \quad x \in \Omega$$

C denotes concentration of red blood cells, and n is a positive constant. The two viscosities were identical at very high rates

$$\lim_{|e_{ij}| \to \infty} \lambda_1 = \lambda_0$$

when the resistance in sliding one fluid plane over another becomes equal to that of deforming a spherical fluid element into an ellipsoidal one of the same volume. If n = 1/2, the constitutive relation, involving shear strength of the suspension in viscometric flow, was shown to be equivalent to the blood flow model of Casson (2).

Using the correspondence principle for viscoelastic fluids, the hysteresis loop determined by Dintenfass was predicted. Its size depends on the relative rates of loading and unloading. The stress component normal to the principal direction and in the plane of flow must be less than the normal stress component in the direction of flow, and both are of higher order smallness when compared with the shearing stress component.

References:

1. Dintenfass, L.: Blood viscosity in healthy men, measured in rhombospheroid viscometer on EDTA blood. Biorheology 11:397-403, 1974.
2. Casson, N.: A flow equation for pigment-oil suspensions of the printing ink type. In: Rheology of Disperse Systems (Edited by Mills, C.C.), Pergamon Press, Oxford, pp. 84-104, 1958.

A NEW NONINVASIVELY OBTAINABLE MEASURE OF CARDIAC CONTRACTILITY BASED ON THE BLOOD PRESSURE DISTRIBUTION IN THE LEFT VENTRICULAR CHAMBER

by

G. Ray
Mechanical Engineering Department
Southern University
Baton Rouge, LA

D.N. Ghista
Spinal Cord Injury Center
VA Hospital
Palo Alto, CA

H. Sandler
Biomedical Research Division
NASA/Ames Res. Center
Moffett Field, CA

BACKGROUND: Current contractility biomechanical measures for the intact left ventricle have been grossly adopted from one-dimensional muscle dynamics; they also entail determination of left ventricular (LV) pressure and geometry, and hence involve invasive procedures.

AIM: This paper provides contractility measures in terms of relative distribution of blood pressure in the LV chamber, at instants during systole.

ANALYSIS: From the cineangiographic or ultrasonic imaging of the dynamic geometry of the LV endocardial outline, the instantaneous LV wall velocities (and hence blood velocities at the endocardial boundary) are obtained. Finite element fluid analysis of the blood flow in the LV chamber, during the small interval of time between consecutive monitored LV frames, yields the relative distribution of blood pressures in the chamber.

RESULTS & IMPLICATIONS: The clinical implementation procedures is non-invasive. A typical graphic display of the blood pressure distribution is shown in the figure. Such a display provides ready, on-line measure of cardiac contracitility, in terms of the ability of the contracting myocardium to generate effective ejection fraction.

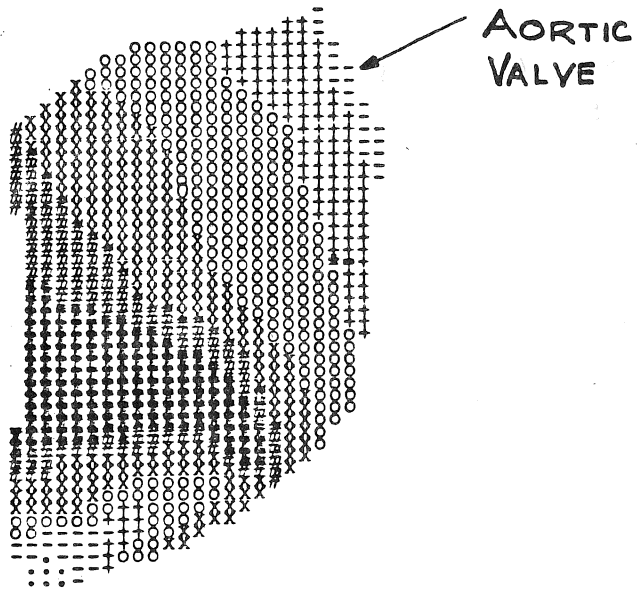

LV PRESSURE GRADIENT

PLASTIC ADAPTIVE RESPONSES OF GAIT THROUGH PREGNANCY: A KINEMATIC ANALYSIS

C. TAVES, J. CHARTERIS
Department of Human Kinetics
University of Guelph
Guelph, Ontario
N1G 2W1

This study investigates the magnitude of specific kinematic adaptations in the human female gait as pregnancy progresses.

Studies of incremental weight gain during pregnancy show that growth curve averages are not always useful in assessing the progress of an individual. Detailed information based on longitudinal data collection constitutes the most reliable method of examining the effect of the prenatal loading. (Ritenbaugh and Quandt, 1978)

The present longitudinal study involved high-speed cinematography of two pregnant subjects, filmed every four weeks through the pregnancy and once per week in the last half of the final trimester. Both the subjects of this investigation were thoroughly conversant with treadmill walking before the onset of pregnancy. Subjects walked on a treadmill at three speeds, randomly ordered for each test. These were 0.6, 0.8 and 1.0 relative speed, a relative speed of 0.8 being equivalent to 0.8 of subject's stature covered in overground distance per second.

The temporal and angular changes were examined on the basis of the month of fetal development as well as weight-gain during the pregnancy. Raw stride-time decreases were seen as the pregnancy progressed although the variability was inversely related to the speed. Time spent in the phase which has the largest base (double support) tended to increase with advancement of pregnancy. The time during which the base of support occupied the smallest area underwent a definite decrease related to advanced pregnancy, suggesting a less confident gait style.

Angle cyclograms of Thigh/Knee, Thigh/Foot and Knee/Ankle were analyzed to show pattern trends. These demonstrate the manner in which the lower extremity accommodated to centre of gravity shifts as the prepartum period shortened. The lower extremity segmental dynamics are discussed in terms of angular and temporal interactions during gait.

In light of the increasing importance of the female's contribution to the economic picture, the recognition and understanding of the adaptive responses of the walking patterns during pregnancy will be considered.

Reference

Ritenbaugh, C., and Quandt, S. Analysis of Incremental Weight Gain during Pregnancy. Presented at the 47th Annual Meeting of the American Association of Physical Anthropologists, University of Toronto, April, 1978.

MECHANICAL EFFICIENCY IN WALKING

M. Y. ZARRUGH

Department of Mechanical Engineering*
The Catholic University of America
Washington, D. C. 20064

The study of power requiremnts and efficiency of human walking provides a basis for evaluating energy needs of prostheses and yields valuable understanding of how muscles do mechanical work in locomotion. Because of the cyclical nature of walking, the net mechanical energy change during any multiple of full cycles is zero. Despite the zero work, muscular effort is still required to bring about the irreversible changes in energy levels. The amount of metabolic power expended during shortening of muscles (positive work) is much larger than that dissipated in the forced lengthening of activated muscles (negative work). Thus, it is customary to assume that all metabolic power is associated with the performance of positive work.

The positive work required to accelerate the body as a whole is determined from the aggregate changes in the energy levels of all segments which are in turn computed from the absolute motions of these segments. The average positive work rate during level walking at free (self-determined) step rates increases with walking speed in essentially linear fashion. At each speed when these work rates are compared to the corresponding total metabolic power expended, a gross mechanical efficiency value results. The efficiency increases rapidly from 9% at the lowest possible speed of 84 cm/s to a maximum of 23% at 170 cm/s. This speed is higher than 132 cm/s for which metabolic energy per unit distance is a minimum. The latter speed is the most likely to be adopted when the subject is allowed to choose his own speed. Thereafter, the efficiency slowly decreases with speed to 18% at the highest possible speed of 235 cm/s.

It is of interest to examine the step rate and step length conditions under which maximum efficiency is achieved at a particular speed. If different step rates are imposed at one constant speed, the average positive work rate remains essentially unchanged at the level required for walking at the free step rate. The constant work rate results in a maximum efficiency at the free step rate, since it requires the least metabolic power.

In conclusion, if no speed is specified, the subject selects a walking speed having the highest efficiency but consistent with minimum energy per unit distance. When the speed is prescribed, the subject adopts a combination of step length and step rate requiring the least metabolic power and hence, having maximum mechanical efficiency.

* Affiliation and address after June 15, 1978 is Department of Mechanical Engineering, University of Michigan, Ann Arbor, MI 48109.

INTERSEGMENTAL RELATIONSHIPS IN HUMAN LOWER EXTREMITY SWING MOTIONS

Sally J. Phillips*, Elizabeth M. Roberts and T. C. Huang
University of Wisconsin - Madison

The study was designed to investigate the influence of non-muscular and muscular forces acting at the knee joint during the swing phase of human lower extremity motion. Special emphasis was placed on the mechanism of knee extension during the swing phase of the run as well as the non-muscular intersegmental relationships which occurred between the thigh and shank.

Newtonian equations of motion for a system of two, linked rigid bodies modeling the thigh and shank-foot were applied to predict the motion of the two segments after the knee muscular force was mathematically considered to be zero. The mathematical details of the prediction model have been reported previously. The prediction model was not intended to simulate real human motion but rather to quantify non-muscular intersegmental relationships and to infer the role of the knee musculature. The behavior of the predicted system depended only upon the kinematics of the hip joint and the musculature crossing the hip joint. The non-muscular influence of the thigh upon the shank was quantified. The predicted motion, with knee forces relaxed, was compared to the kinematic and kinetic parameters in the observed motion, with knee forces operant. The latter were calculated by cinematographic techniques. The differences in the behavior of the thigh and shank between the observed and predicted motions were attributed to the musculature crossing the knee joint.

The knee musculature was released at several different time points during the swing phase of the run, the speed of which was equivalent to a 4-minute mile. The motion of the thigh has a direct, causal relationship to the motion of the shank in the predicted motion. The influence of any given thigh motion upon the shank is somewhat dependent upon the shank kinematics at the time of knee musculature release.

As the moments of force acting on the thigh increased thigh forward rotational speed, the speed of knee flexion increased in the predicted motion. When the thigh moments of force decreased the speed of thigh forward rotation, knee extension was facilitated. In this case the thigh motion was quantitatively shown to either slow knee flexion or speed knee extension. The non-muscular forces acting at the knee joint produced moments which accelerated the shank forward. Although this relationship between the thigh and shank motion was previously suspected, quantitative evidence was not available. Furthermore, the role of the knee musculature in producing observed knee angular velocity may have been overemphasized; a substantial amount of knee extension can occur without the aid of the musculature crossing the knee joint. When the speed of thigh backward rotation increased, the speed of knee extension also increased; the greatest negative thigh acceleration was associated with the greatest angular acceleration for knee extension as well as the largest resultant forces at the knee joint. Decreasing the speed of backward thigh rotation decreased the speed of knee extension.

The quantification of non-muscular intersegmental relationships can answer questions concerning the non-muscular contribution of proximal segment motion to distal segment motion. The data suggest that the non-muscular interrelationships can play a substantial role in knee extension during lower extremity swing motions.

---

*Present address: Department of Physical Education, University of Maryland, College Park, Maryland 20742

EVALUATION OF ADULT CLASPING FORCES ON AN UNRESTRAINED, LAP-HELD, INFANT DUMMY.

Dinesh Mohan+ and Lawrence W. Schneider*

Every year hundreds of young children are killed and thousands injured in motor vehicle crashes. Although many of these deaths and injuries can be prevented with the use of child restraint systems, the vast majority of parents do not choose to do so. Williams (1) reports that holding a child in one's arms or lap is potentially lethal if a crash occurs, yet many adults continue to transport children in their laps. Furthermore airline regulations require that infants be held in adults' arms in the airplane rather than be restrained by adequate restraint systems. The experiments described in this paper were performed to measure the maximum forces that adults can exert in holding an 8.5 kg infant dummy (age 6 months) in their laps. Both quasi-static and dynamic tests were conducted.

Three male and three female parents of young children were tested. In the quasi static tests the dummy was pulled away from the adults, who were restrained in their seats by lap and shoulder belts, at nominal velocities of 0.05 m/sec and in the dynamic tests at 2.5 m/sec. The restraining forces were measured by measuring the tension in the cable attached to the dummy.

The results from the dynamic and quasi-static tests indicate that the maximum forces that lap and shoulder belted adults can exert in holding an infant dummy in their laps are far less than the inertial force that would be exerted by an 8.5 kg infant decelerated at more than 30 G's. This means that in a motor vehicle barrier crash at 50 Km/hr, an infant held tightly by a restrained adult would almost certainly strike the dash or windshield. Similarly in airplanes, in crash or turbulance situations, the infant is likely to hit the hard structures around it. Therefore, it is not safe for infants to be transported in adults' laps in automobiles or airplanes even in the relatively rare instances that the adults are restrained.

1. Williams, A. F. "Warning: In Cars, Parents May Be Hazardous to Their Children's Health." Insurance Institute for Highway Safety, Washington, D.C., 1978.

+Research Department, Insurance Institute for Highway Safety, Watergate 600, Washington, D.C. 20037

*Biomedical Department, Highway Safety Research Institute, The University of Michigan, Ann Arbor 48109

TITLE: An Anthropometric Dummy to Evaluate Ski Equipment

AUTHOR: George Raskulinecz and Eugene Bahniuk
Orthopedic Engineering
Case Western Reserve University
Cleveland, OH 44106

A dynamic testing method has been designed and implemented to evaluate the performance of ski bindings, ski boots, skis and related equipment. The device consists of an anthropometric dummy of the 50th percentile skier. It has the same mass, center of gravity and moments of inertia about its principle axes as does a skier in a crouched position. The dummy is articulated in such a way as to mechanically reproduce the spring rates in torsion and bending of the foot, ankle, tibia, knee and femur. Thus, during a simulated ski accident, the dummy skier imposes the same passive loads on an unmodified boot, binding and ski assembly as would a live skier. The live skier could also contribute a variable active load due to musculature and reflexes. The long bones of the lower limb are modeled by a steel column load cell having six strain gage bridges. These yield a measurement of the three forces and three moments which act on the "lower extremity" of the dummy.

The dummy skier is used in conjunction with a dummy ski slope. This consists of a plywood and styrofoam panel with an aluminum frame. It measures 8 ft. x 8 ft. and weighs 170 pounds. It is constrained to move in horizontal plane by a pair of 16 ft. rails. It can be accelerated to 44 ft. per second within one foot by means of a hydraulically actuated cable and pulley system giving it a stroke of 8 ft. The surface of this sled is covered with an Astroturf-like artificial snow. It is drawn beneath the dummy skier recreating the movement of a skier on the slope. A variety of accidents can be simulated by arranging racing poles, simulated moguls, etc., on the sled in the path of the dummy skier.

Preliminary tests have shown the dummy skier to produce data that agree with the moderate and high speed test data of the standard ASTM ski binding test machine. Due to its inertial loading method, it does not perform the static or very slow test commonly used to evaluate bindings per ASTM method. However, it can more easily replicate typical ski accidents where the loading configuration of the ASTM machine must be a complex approximation derived from a careful analysis of the accident. An appropriate feature of the ASTM machine is that the ski boot is modified to approach infinite rigidity relative to the binding under test and is attached to what the binding regards as a skier of infinite proportions. Our test with the anthropometric dummy indicate that the rigidity of the ASTM machine is a reasonable approximation.

EFFECTS OF HELMET INERTIA AND RESTRAINING COLLARS ON HEAD/NECK DYNAMICS

Ronald L. Huston
Professor of Mechanics
Department of Engineering Science
Loc. #112
University of Cincinnati
Cincinnati, Ohio 45221

and

Joseph Sears
Research Assistant
Department of Engineering Science
Loc. #112
University of Cincinnati
Cincinnati, Ohio 45221

ABSTRACT

It has been suggested in many discussions that the crash helmet while protecting against direct-impact injury, may however, actually contribute to indirect-impact (e.g. whiplash) injury due to the added mass on the head/neck system. It has been suggested that it is possible to reduce this indirect-impact injury hazard while retaining the beneficial protection against direct-impact, through use of helmet restraining devices. Specifically, it has been suggested that the helmet/head motion may be restrained during periods of high acceleration by an inflatable air bag collar and resisting stops. It has been further claimed that such restraining devices could reduce the indirect-impact injury hazard to below the hazard level associated with no helmet at all.

It is the objective of this paper to quantitatively examine the feasibility and validity of these claims using the recently validated UCIN Head/Neck computer simulation code. Specifically, the head/neck dynamics are computed and compared for the following three cases: 1) No helmet or protective devices, 2) Helmet without restraining devices, and 3) Helmet with restraining devices. These comparisons are made using a deceleration profile for which the UCIN code has been validated with live experimental data. The results show that the proposed restraining devices do indeed provide potential protection against direct-impact (e.g. whiplash) injury.

EXPERIMENTAL ANALYSIS OF THE VIBRATIONAL CHARACTERISTICS OF THE HUMAN SKULL

Tawfik B. Khalil
Biomedical Science Department

David L. Smith
Fluid Dynamics Research Department

and

David C. Viano
Biomedical Science Department

General Motors Research Laboratories
Warren, Michigan 48090

ABSTRACT

Analytical models of the human skull structure have generally represented the gross geometric and material characteristics; however, a model should also have accurate frequency response characteristics since these are essential for collision and head injury analyses. An experimental investigation was conducted to identify the dynamic characteristics of freely vibrating human skulls. Resonant frequencies and associated mode shapes in the frequency band from 20 Hz to 5000 Hz were delineated for two dry human skulls. Osteometrically, one skull corresponds to a 50th percentile male skull (skull 1) and the second is representative of a 5th percentile female skull (skull 2).

Digital Fourier analysis techniques were used to identify the resonant frequencies and mode shapes of each skull. Eleven resonant frequencies were identified for skull 1, with the lowest being 1385 Hz. In contrast, skull 2 exhibited only 6 resonant frequencies with the first being 1641 Hz. Nine mode shapes were identified for skull 1, but only 5 modes for skull 2. The vibrational pattern of the human skull as indicated by its mode shapes seems to be a unique property of that skull. Skull sutures did not appear to influence the modal pattern of the skull. The uniqueness of each skull's vibrational characteristics suggests that additional skulls should be studied before a universal analytical model is attempted to be developed.

STIFFNESS OR EXTENSIBILITY OF INTERTIDAL KELP: A COMPARATIVE STUDY OF MODES OF WITHSTANDING WAVE ACTION

M. A. R. Koehl
Division of Biology and Medicine, Brown University
Providence, Rhode Island, 02912

Most sessile marine organisms in areas subjected to wave action avoid large drag forces because they are short and squat or are hidden in holes or behind protrusions. In contrast, tall sessile organisms such as large algae face rapid flow in wave-swept areas. Mechanics can be applied in studying adaptations of such large organisms that allow them to withstand waves.

I conducted a comparative study of the large kelp Lessonia nigrescens and Durvillea antarctica which form a conspicuous belt in the low intertidal zone of wave-beaten rocky shores in Chile. I surveyed the distribution and modes of mechanical failure in nature of these plants, observed their behavior in waves, and measured current velocities over, drag forces on, resistance to bending of, and gross morpholoigcal features of the plants in situ. I also conducted stress-strain and creep tests in the laboratory.

Lessonia have "woody" branching stipes which hold their numerous strap-like fronds about 0.5m above the substratum whereas Durvillea have short (0.1m) unbranched stipes and thick, spongey blades up to 10m long. Both species are exposed to waves with peake velocities between 1 and 6m.s^{-1} and experience drag forces of the order of 0.2 to 20N under non-stormy conditions. Form drag is minimized on these flexible plants which are bent over parallel to the flow, however, about five times the force is required to bend a Lessonia stipe a given amount than a Durvillea stipe. The elastic modulus of Lessonia stipe ($\bar{x}$ = 22.0MN·m^{-2}) is greater than that of Durvillea stipe ($\bar{x}$ = 3.5MN·m^{-2}) and blade ($\bar{x}$ = 0.9MN·m^{-2}) (see typical stress-strain curves below). Although breaking stress for Lessonia stipe ($\bar{x}$ = 1.2MN·m^{-2}) is nearly twice that of Durvillea stipe ($\bar{x}$ = 0.7MN·m^{-2}), the stresses they normally encounter in situ are only of the order of 0.01 to 0.1MN·m^{-2}. Durvillea extend much more before breaking (breaking strain for blades, $\bar{x}$ = 0.35; stipes, $\bar{x}$ = 0.17) than Lessonia (breaking strain for stipes, $\bar{x}$ = 0.09), hence the work that waves must perform to break either species is essentially the same (4KJ·m^{-2} in 5.4cm long specimens). Both species tend to break at flaws produced by grazing animals, although this effect is more pronounced in the long-lived Lessonia than in Durvillea, which are extensively harvested by man.

Durvillea and Lessonia illustrate two basic strategies of large sessile organisms to withstand waves: being flexible and extensible, or being stiff and strong.

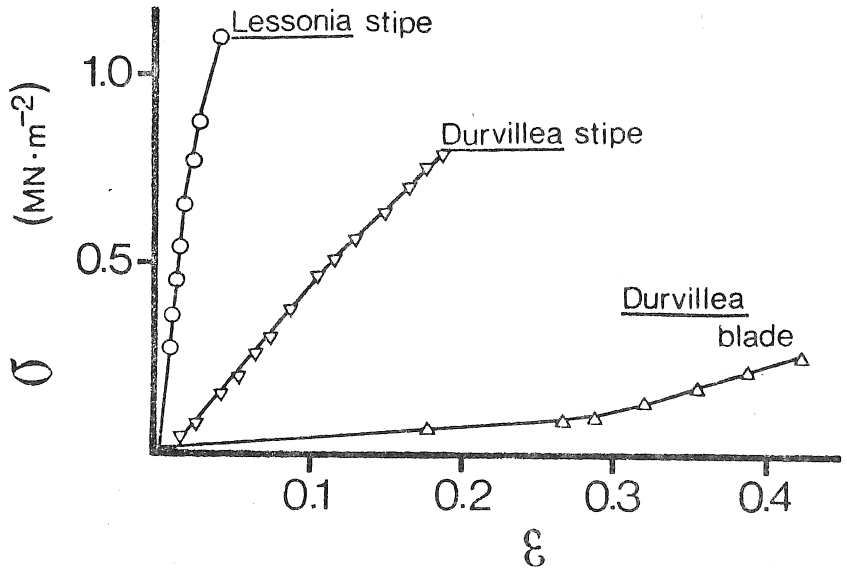

CROSS-SECTIONAL AREA MEASUREMENT OF THE CRUCIATE LIGAMENT: EVALUATION OF ITS PRESSURE DEPENDENCE

ALLARD, P., THIRY, P.S. and DROUIN, G. - Biomedical Engineering Programme, Ecole Polytechnique, Montréal, Québec, Canada.

This study is part of a research programme dealing with the characterization of the mechanical behaviour of the canine lateral cruciate ligament within its functional physiological range (Dorlot, J.M. et al. - 1978).

The intricate geometry of the cruciate ligament and the lack of adequate description of the methods used to obtain its cross-sectional area have complicated the normalization of the load-elongation data in terms of stress and strain respectively. Ellis (1969) has reported that the measurements taken with an area micrometer were "considerably influenced by the pressure applied to the specimen". Recently, Noyes et al. (1976) have used a similar technique where a single blade pressure of 0.12 MPa was applied to measure the ligament cross-sectional area in Rhesus monkeys and humans.

To establish a basis for the choice of an optimal cross-sectional area measurement method for the canine cruciate ligament, an experimental study was undertaken. Its main objectives were to quantify the cross-sectional area dependence on the pressure and select the most appropriate pressure.

Method

Ten canine preparations were studied with a non-rotating spindle blade micrometer (Mitutoyo, 122) whose thimble breakaway torque develops a constant force of 1.96 N. By the use of matching pairs of plexiglass blocks of various widths, the applied pressure on the ligament could be varied between 0.04 and 0.25 MPa.

Results and Discussion

The ligaments were preconditionned by compressing them ten times at a pressure of about 0.04 MPa prior to the experiments. This procedure was introduced following the observation of a drop of 8 to 15% in the first two cross-sectional area measurements as compared to all the remaining ones.

For each ligament, the values obtained for the areas were normalized with respect to the smallest area and plotted as a function of the applied pressure. Data from all the ligaments were reduced to a single curve which illustrates a decrease in the normalized cross-sectional area by 25% for pressures ranging from 0.04 to 0.16 MPa. For all pressures between 0.16 and 0.25 MPa the normalized cross-sectional area remained constant.

References

1. Dorlot, J.M., Beaulne, R., Ait Ba Sidi, M., and Drouin, G. (1978). Functional and Dynamic Characterization of Canine Lateral Cruciate Ligaments. Proceedings 1st International Conference on Mechanics in Medicine and Biologic, Aachen, Germany.

2. Ellis, D.G. (1969). Cross-sectional Area Measurements for Tendon Specimens: A Comparaison of Several Methods. Journal of Biomechanics 2, 175-186.

3. Noyes, F.R. and Grood, E.S. (1976). The Strength of the Anterior Cruciate Ligament in Humans and Rhesus Monkeys. Journal of Bone and Joint Surgery, 58-A, 1074-1082.

Acknowledgements

This project was sponsered in part by the National Research Council of Canada.

Biomechanical Modeling of Tendon During Wound Healing

Bruce Goldin, Ph.D., Department of Orthodontics, University of Connecticut, School of Dental Medicine, Farmington, Connecticut 06032

The process of wound repair involves the restoration of form and strength to the injured part. Previous studies on regenerating tendon have been mainly biochemical and histological while biomechanical characterization has been limited to measurement of tensile strength.

The purpose of this study was to obtain reproducible, good quality cicatrized New Zealand rabbit extensor digitorum communis tendon from the fifth through thirteenth post-surgical day, characterize the biochemical, physical, and mechanical properties during the healing process, and determine if any relationship might exist between the physical or mechanical variables and the tendon biochemical composition. In order to achieve a consistent initial gauge length and provide direct measurement of the mechanical properties of healed tendon a method of tendon splinting was developed. The physical measurements (dry weight and cross-sectional area), mechanical testing by isometric thermic denaturation (shrink temperature, denaturation curve slope, thermic yield tension, maximum thermic tension), and biochemical assay of tendon and physiological saline bathing medium (collagen, acid mucopolysaccharides) were used to determine the rate and quantity of protein and ground substance formed and the quality of molecular cross-linking. Temperature change during hydrothermal shortening was at a rate of 2°C/minute commencing at 40°C past the shortening temperature to maximum contraction and subsequently to failure.

The results of this study indicate that physical and mechanical property changes during the fifth through thirteenth post-surgical day occur concurrently with the biosynthesis of collagen and acid mucopolysaccharides. The shape of the isometric thermic denaturation curve for the wounded tendon group was bimodel differing from the intact tendon group. A multiple linear regression mathematical model was developed reflecting the correlation of biochemical and biomechanical factors. The model described the physical and mechanical property changes in the healing tendon, represented as a constitutive equation having coefficients which were function of treatment, time, and several tissue biochemical components. It provided values for physical and mechanical property changes utilizing differences associated with treatment and length of healing period, along with the selected biochemical covariates of hydroxyproline, protein, and hexosamine concentration levels. Application of the biochemical values to the model estimated the physical and mechanical properties of the wounded group well when differences in the property changes between the wounded group and the intact group were large. When treatment effects were small, both groups were predictable.

Since mechanical resistance of collagen fibers depends on all, or most, of the chemical properties, monitoring the biochemical composition of the structural protein might be a valuable aid in the proper maintenance of normal tissue growth or elucidating the genesis and progression of a disease. Use of a mathematical analog to relate tissue structure to function provides an additional tool to study the intricate process of connective tissue remodeling. Application of the model may allow a proper prescription of therapies to increase the precisely timed formation of biochemical constituents to accelerate the wound healing process.

Stereometrical and Mechanical Characteristics of Porcine Aortic Valves

Yannis F. Missirlis and Ming Chong
Department of Engineering Physics
McMaster University, Hamilton, Ontario
Canada

A new methodology has been developed whereby the inhomogeneous and anisotropic aspects of an irregularly surfaced organ component have been incorporated in establishing the material properties of this tissue.

Specifically the direction-dependent post-transition elastic moduli have been calculated from microtensile experiments for the porcine aortic valve leaflets with an average of $E_{CIRC}/E_{RAD} = 3.2$. Furthermore pressure-strain data have been measured for a grid of points on the surface of a porcine aortic valve and an isostrain map has been developed for P = 80 mm Hg.

The stress analysis of the porcine aortic valve leaflets in diastole at 80 mm Hg pressure in-vitro is presented. Incorporation of local geometrical asymmetry, material inhomogeneity, anisotropy and non-linearity are applied. The stress theory used is a modified form of the thin membrane stress theory for a homogeneous, linearly elastic and orthotorpic lamina. Modifications are made so that the Hooke's Law constitutive equations of stress may be applied to the inhomogeneous, non-linearly elastic and orthotropic thin (membrane) aortic valve leaflets.

Stress calculations are made on the premise that the valve is in pre-transition (i.e., low elastic modulus) in the circumferential direction and post-transition (i.e., high elastic modulus) in the radial direction. It is shown that $\sigma_{CIRC} < 1$ gm/mm^2. For most of the noncoronary leaflet, $0 < \sigma_{RAD} < 30$ gm/mm^2. The areas of highest stress concentrations are in the areas of mutual leaflet coaptation near the Node of Arantii. A progressive increase of radial stresses from the sinus-annulus edge toward the node is observed.

The isostrain and isostress mapping thus developed for the natural porcine aortic valve provides on the one hand a valuable tool for the study of other heart valves and of other organs as well, and on the other, forms the basis for optimized treatment and processing of the glutaraldehyde-treated porcine aortic valves. The latter have been clinically used by the thousands in the past 3 years without, however, a thorough investigation of their mechanical and functional properties being reported.

PATHOMECHANICS OF ULNAR DRIFT:

THE ROLE OF THE FLEXOR TENDONS TO THE LITTLE FINGER

James R. Buchanan, M.D.
Division of Orthopaedic Surgery
The Milton S. Hershey Medical Center
of The Pennsylvania State University
Hershey, PA
17033

A previously unexplored aspect of ulnar drift is analyzed by theoretical free body techniques. The extrinsic flexor tendons to the little finger enter the fibro osseous canal at the metacarpal head from a radial and proximal direction. During grasp, after excursion of the metacarpophalangeal, proximal interphalangeal and distal interphalangeal joints is complete, the component of the flexor tendon tension perpendicular to the axis of the fifth metacarpal causes supination of the metacarpal. This assertion was proven by loading the profundus tendon to the little finger of a hand mounted on a frame, and observing the rotation of the metacarpal. Supination of the proximal phalanx is resisted by forces transmitted from the thumb through the fingers to the radial aspect of the little finger.

Free body analysis of the proximal phalanx with the metacarpophalangeal joint flexed to 90 degrees demonstrates that, under this loading condition, tension is generated in the radial collateral ligament and a compression force is generated between the metacarpophalangeal joint surfaces on its ulnar side. Radial collateral ligament tension stress in the course of normal hand use accounts for its susceptibility to mechanical failure when exposed to lytic enzymes in the rheumatoid hand. Ulnar drift of the phalanx follows failure of the radial collateral ligament.

Radial deviation of the metacarpals and collapse of the carpus, two frequently associated abnormalities in the rheumatoid hand, increase the magnitude of the transverse component of the flexor force on the metacarpal and thereby augment the tendency to ulnar deviation.

AN INVESTIGATION OF CARPAL BONE MOTION USING A THREE DIMENSIONAL SONIC DIGITIZER

Richard A. Berger, Youngil Youm, and Adrian E. Flatt
The University of Iowa, Iowa City, Iowa

The wrist (carpus) is a complex joint with eight carpal bones arranged in two rows of four bones each (Fig. 1). To date, analysis of carpal bone motion has been limited to gross visual observation and radiographic studies. The methodology for a more accurate analysis of individual carpal bone motion has been developed.

A sonic digitizer system (Graf/Pen sonic digitizer interfaced with a PDP-12 computer) is utilized for the experimental and analytical investigation of carpal bone motion in fresh cadaver specimens. This system includes three orthogonally oriented linear microphones, two sets of three noncollinear spark gaps mounted on lightweight frames, and control systems. When commanded, a spark arcs across each gap producing a high frequency sound that is localized by the microphones.

The cadaver specimen is rigidly fixed in neutral forearm rotation, and the five prime wrist tendons are statically loaded. The carpal bone to be studied is exposed and a spark gap set is fixed to it with a threaded Kirschner wire. All soft tissues are repaired, and the intracapsular wrist ligaments are not compromised by the dissection. The second spark gap set is fixed to the distal radius diaphysis and serves as a reference. The wrist is then passively moved through a planar constrained arc of flexion-extension motion and radial-ulnar deviation. Throughout these arcs of motion, the spark gaps sequentially pulse at 0.15 second cycles. The position of each pulse is digitized in reference to the microphone coordinate system. From this data, a computer program produces a three dimensional kinematic analysis of the carpal bone studied during the wrist motion.

Orthogonal biplanar x-rays are taken of the specimen with the spark gap sets in situ in order to transform the sonic digitizer data to an anatomic coordinate system. The origin of this system is the wrist center of rotation, which is located in the head of the capitate (Figs. 2 and 3).

This methodology is an accurate laboratory tool for determining the carpal bone kinematics in normal and diseased wrists.

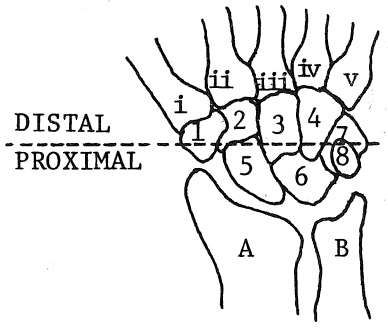

Fig. 1

A:Radius
B:Ulna
i-v:Metacarpals
1:Trapezium
2:Trapezoid
3:Capitate
4:Hamate
5:Scaphoid
6:Lunate
7:Triquetrum
8:Pisiform

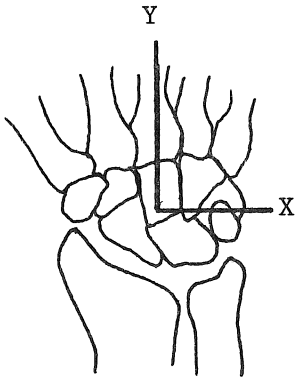

Fig. 2

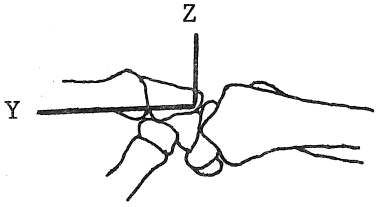

Fig. 3

A NON-DESTRUCTIVE METHOD FOR EVALUATING THE BODY GEOMETRY AND ITS PHYSICAL PROPERTIES*

H.K. Huang, F.R. Suarez, M.J. Cerroni, O.T. Steiner, D.D. Robertson
Georgetown University Medical School, Washington, D.C. 20007

L. Ovenshire
National Highway Traffic Safety Administration

In biomechanics research it is often necessary to obtain the body geometry and the corresponding physical properties of the specimen under consideration. The conventional methods for evaluating these parameters are multi-plane X-ray images and segmented trunks; however, the former technique provides only crude estimations of body geometry while the later is destructive. In any case, neither method reveals accurate information concerning tissue structures or mass density distribution.

The purpose of this paper is to report on a non-destructive method for evaluating these parameters utilizing the computerized tomograhic (CT) scanning technique. The CT procedure, which was developed in 1974 and has been widely used as a radiographical diagnostic technique, is relatively noninvasive and gives high-contrast spatial and density cross-sectional images of the object under investigation. Our research goal is to use the CT method to generate from cadaveric scans a comprehensive data base of three-dimensional geometry and physcial properties of human bodies. This method can also be used to generate similar information from live volunteers or patients with only a minimum X-ray dosage to the participants.

The major steps, at this stage for carrying out this research project are as follows:

1) Acquiring and Preparing a Cadaver
2) Scanning the Cadaver
   The specimen is placed in a supine position on the CT scanner. Beginning at the cranium and ending at the ankle joints, scans are taken at one centimeter intervals. It takes 30 seconds to complete one cross-sectional scan.
3) Obtaining Three-Dimensional Body and Anatomical Componenet Geometry
   Three-dimensional body and anatomical component geometry of a specimen can now be obtained from the scans. Since the CT scans are already in a digital format, it is not necessary to digitize the scan pictures. External body contours and boundaries of anatomical structures can be obtained using standard pattern recognition computer programs. Some examples of cross-sectional scans and their boundaries and skeletal structures are shown in the Figure.
4) Computing the Mass, Center of Gravity and Inertial Tensor for Body Sections and Anatomical Components
   Standard computational methods can be used to obtain these parameters from each cross section.

The human body data base generated by this method will be a comprehensive one, and the format will be self-explanatory with easy access for researchers in any branch of the biomechanics field.

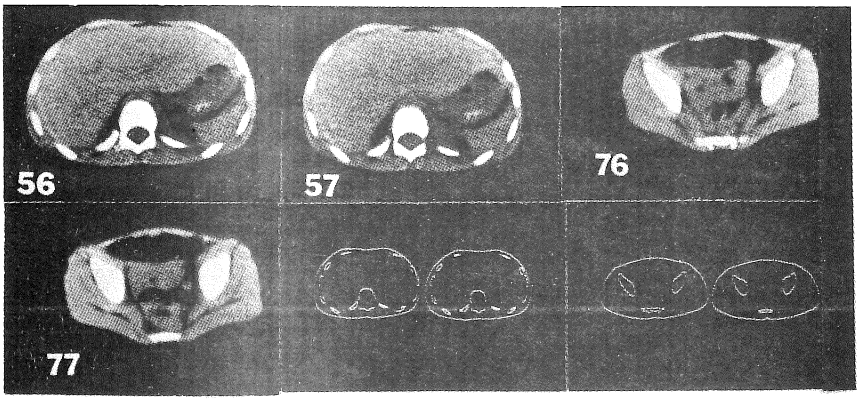

* This research is supported by the Department of Transportation (Contract Number DOT-HS-7-01661)

PREDICTING TOTAL BODY VOLUME IN DIFFERENT SIZE MALES USING A GENERALIZED MODEL

In the present study a theoretical model is proposed for calculating total body volume for the human body using 3 geometric shapes representing 10 different body segments. A unique feature includes a " rounding-off " procedure for the trunk segments; this is a mathematical technique whereby right-angled shapes are rounded-off so as to more closely conform to actual body contours.

Sixty-three males (mean age 30.3 yrs. $\pm$ 1.01 S.E.) were divided into small, medium, and large sizes using a bivariate sizing scheme based on height and weight. Most heights and lengths, and some breadths, depths, and circumferences were significantly different ($p < .05$) between the different groups. The prediction of body volume was highly correlated with densiometrically determined body volume ($\underline{r}$ = .98 S.E. = 2.9% of mean) for the total group. The model was shown not to be size specific as the validity coefficients were $\underline{r}$ = .97 (S.E. = 2.6% of mean), $\underline{r}$ = .96 (S.E. = 3.0% of mean), and $\underline{r}$ = .99 (S.E. = 2.6% of mean) for the small, medium, and large groups, respectively. In view of these high validity coefficients it was concluded that the summation of the segmental geometric shapes for calculating volume closely approximated the actual total body volume. Therefore, utilization of these segmental shapes is proposed in the computation of biomechanical properties (moment of inertia, radius of gyration, etc.) during kinetic analysis.

Stan Sady
Patty Freedson
Victor L. Katch

Physical Performance Research Laboratory
Physical Education Department
401 Washtenaw Ave.
C.C.R. Bldg.
The University of Michigan
Ann Arbor, Michigan 48109

Force and Impact Determinations of Certain Karate kicks

by
Laurence Gray
Dr. John Melvin
Dr. Ruth Harris

In order to examine injury potential, a series of karate kicks to the chest were analyzed. The kinematic differences of the karate kicks as well as the forces generated were also examined.

Methods-In one set of tests, a series of three different kicks were made, by an expert in Korean Karate, to the chest of an anthropometric test dummy having realistic biomechanical responses. The dummy was equiped with a triaxial accelerometer set in the chest.The kicker's leg was targeted for motion analysis with high speed film. A separate series of kicks was made against a padded load cell to measure the direct force capability of the kicker.

Results-Based on the analysis of the test data the following factors were determined:
Mass of the impacting kick was determined to be mass of the right leg, calculated at 34.54 lbs. Kick terminal velocities, measured on film, ranged from26.1 ft./sec. to 36.7 ft./sec.(17.8-25.1 MPH), depending on the type of kick analyzed. Impact dummy resultant acceleration varied from 19.5-29.6 G's, and kick force as measured on the force transducer ranged from 625-2200 lbs. of force generated.

It was concluded that certain karate kicks, when compared with blunt chest impactions found in automobile chest impact studies, can result in severe chest injury.

Author's Address:
Laurence Gray
1032 Michigan Ave.
Ann Arbor, Michigan 48104

Assistance:
Dr. John Melvin
The University Of Michigan
Highway Safety Research Institute
Huron Park and Baxter Road
Ann Arbor, Michigan 48109

Dr. Ruth Harris
The University of Michigan
Department of Physical Education
401 Washtenaw Avenue
Ann Arbor, Michigan 48109

Analysis and Model of the Handspring Vault

A. Dainis

Biomechanics Laboratory
Department of Physical Education
University of Maryland, College Park, Md. 20742

In the sport of gymnastics the handspring is the basis of all the advanced vaults, and is therefore of considerable interest to all coaches, teachers, and competitors. Compared to other movements it is quite simple in nature, being a purely sagittal motion capable of being represented by a one, two, or three link system for the accomplished performer.

This study analyses, from cinematographic records, the performance of a number of female gymanasts of various skill levels, and investigates the take-off parameters (velocity and angular velocity), horse contact (force, duration, impulse, energy loss), and after-flight parameters, with a view of identifying an accurate model for the action. Of particular interest is the horse-body interaction, the modelling of which would enable the outcome of the vault to be predicted from three take-off parameters. It would then be relatively straight forward to calculate the take-off parameters necessary for an optimum vault.

It was found that the free flight phases can be modelled quite easily, but the interaction phase cannot be represented by a simple spring system, and generally involves some loss of energy of the body. Poor vaulters do not generally achieve sufficient angular momentum during take-off and therefore remain in contact with the horse for a longer period of time. This causes a delay of the repulsion and a loss of energy stored in the deformed horse-body system.

The interaction of the human body with semi-rigid supports, especially where large forces are involved, is quite common and of vital interest to persons concerned with safety, teaching and performance of sports skills. Since direct measurements in these situations is usually very difficult, the use of realistic models is an attractive alternative.

OPTIMIZATION OF THE STANDING VERTICAL JUMP

by
Y. S. Yoon, J.G. Andrews and Y. Youm
College of Engineering, University of Iowa, Iowa City, Iowa 52242, USA

ABSTRACT

The purpose of this investigation is to determine the kinematic behavior of a mechanical system that will optimize a particular objective function or performance index. This problem is solved for a simple four-bar planar open linkage system representing the human body during a standing maximal vertical jump. Bilateral symmetry is assumed, and the body is modeled as four rigid segments (head and trunk, upper extremities, thighs, and lower legs plus feet) interconnected by smooth pin joints. The overall jumping motion is divided into a pre-flight phase and a flight phase, with the vanishing of the foot-ground contact force determining the transition time between phases. Newton's equations of motion are written for each segment in terms of the forces and moments exerted at the joints.

A nonlinear programming problem is formulated where the objective function is the maximum height reached by the distal tip of the upper extremity segment. The four segmental angular accelerations are chosen as design variables, and the four corresponding initial angular orientations are included as design parameters. An additional dummy design variable is used for computational convenience during the flight phase in order to make the number of configurational variables the same during each phase of the motion. Appropriate constraints are placed on the dummy independent variable, the joint angles, and the muscle torques at the joints.

An optimal solution to this constrained nonlinear programming problem is found using the method of steepest descent. Once the optimal angular accelerations are determined, the associated kinematic behavior of the open linkage system and the optimal joint torques are easily determined. Numerical results are presented using body segment parameters for a typical adult male and reasonable constraint values.

The methodology presented is sufficiently general and efficient to facilitate the determination of those particular human body motions that optimize a wide variety of performance criteria.

Trajectory Corrections Using Rotational Energy

Jerome V. Danoff, Ph.D.
Department of Rehabilitation Medicine

Paul A. Anderson, M.A.
Department of Physical Therapy
University of Maryland
School of Medicine
Baltimore, Maryland 21201

The task for this study was a novel motor skill involving a backhanded ball toss at an inclined target with the arm moving in a sagittal plane. A small cup attached to the subject's wrist held the ball at the start of movement and until the ball eventually flew out of the cup towards the target. Cinematographic data were collected on arm angle and angular velocity at the moment of ball release. The target was marked with horizontal bands, and analysis of the trajectory pathway resulted in theoretical target impact levels based on ball release angle and velocity. Observed target impact, however, was consistently lower than theoretical values which led to the view that not all of the ball's kinetic energy was contributing to translation. Subsequent corrections were made to the theoretical equations to account for trajectory energy loss due to rotation of the ball, and these corrected values more closely agreed with the observed impact levels. Higher order corrections still may be necessary for complete agreement in trajectory analysis.